Bull Earthquake Eng
DOI 10.1007/s10518-014-9669-y

ORIGINAL RESEARCH PAPER

Investigation of the characteristics of Portuguese regular moment-frame RC buildings and development of a vulnerability model

Vitor Silva · Helen Crowley · Humberto Varum · Rui Pinho · Luis Sousa

Received: 13 April 2013 / Accepted: 31 August 2014

Abstract A vulnerability model capable of providing the probabilistic distribution of loss ratio for a set of intensity measure levels is a fundamental tool to perform earthquake loss estimation and seismic risk assessment. The aim of the study presented herein is to develop a set of vulnerability functions for 48 reinforced concrete building typologies, categorized based on the date of construction (which has a direct relation with the design code level), number of storeys (height of the building) and seismic zonation (which affects the design of the buildings). An analytical methodology was adopted, in which thousands of nonlinear dynamic analyses were performed on 2D moment resisting frames with masonry infills, using one hundred ground motion records that are compatible, to the extent possible, with the Portuguese tectonic environment. The generation of the structural models was carried out using the probabilistic distribution of a set of geometric and material properties, compiled based on information gathered from a large sample of drawings and technical specifications of typical Portuguese reinforced concrete buildings, located in various regions in the country. Various key aspects in the development of the vulnerability model are investigated herein, such as the selection of the ground motion records, the modelling of the infilled frames, the definition of the damage criterion and the evaluation of dynamic (i.e. period of vibration) and structural (i.e. displacement and base shear capacity) parameters of the frames. A statistical bootstrap

V. Silva (✉) · H. Varum
Civil Engineering Department, University of Aveiro, Aveiro, Portugal
e-mail: vitor.s@ua.pt

V. Silva · H. Crowley · R. Pinho
GEM Foundation, Pavia, Italy

H. Varum
Faculty of Civil Engineering, University of Porto, Porto, Portugal

R. Pinho
Civil Engineering and Architecture Department, University of Pavia, Pavia, Italy

L. Sousa
Faculty of Civil Engineering, University of Porto, Porto, Portugal

Published online: 11 September 2014

method is demonstrated to estimate the variability of the loss ratio at each intensity measure level, allowing the estimation of the mean, as well as 10 and 90 % percentile vulnerability curves.

Keywords Exposure · Vulnerability · Portuguese building stock · RC structures · Structural modelling

1 Introduction

Earthquake loss estimation can play a fundamental role in the sustainable development of a given region, providing local governments and other decision makers with valuable information necessary for the creation of risk mitigation actions. These may include post-disaster emergency planning, building retrofitting campaigns, creation of insurance pools, strategic urban planning, amongst other measures. An important component for this purpose is a vulnerability model that allows the estimation of losses from structural/non-structural damage due to earthquakes, as a function of a set of ground motion parameters.

The structural vulnerability of the Portuguese building stock has been the target of only limited investigation in recent years. Oliveira et al. (2005) characterized the physical vulnerability of the Portuguese building stock using two methodologies: one based on the vulnerability curves developed by Coburn and Spence (2002) in terms of macroseismic intensity; and a second method in which vulnerability indexes were determined for each building typology, and combined with the formulae proposed by Lagomarsino and Giovinazzi (2006) to estimate mean damage curves, also using macroseismic intensity. These models were employed in a scenario assessment for Lisbon, resulting in collapse maps for two historical earthquakes.

In the European project LESSLOSS (2004–2007) (Calvi and Pinho 2004), in which the metropolitan area of Lisbon was used as a test case (Spence 2007), various fragility functions developed by Carvalho et al. (2002) were used to investigate the seismic risk for this region. These curves were computed using the simplified methodology from HAZUS (FEMA 1999) that relies on a capacity curve that is constructed from a group of parameters (related to the design of the structure), which is then used to extract a set of spectral displacements (one per limit state) according to pre-defined global drift thresholds. Each spectral displacement is used as the median of a cumulative lognormal distribution, with a given pre-established logarithmic standard deviation, to represent the respective limit state fragility function. For each building typology, a number of curves describing the probability of exceeding a set of damage states was computed, using damped spectral displacement at the inelastic period to represent the various levels of ground motion. Such output can be used together with capacity spectrum-based methodologies (e.g. N2—Fajfar 1999; Capacity Spectrum Method—Freeman 2004) to assess the distribution of buildings throughout a set of damage states, which can then be converted into an economic loss.

Notwithstanding the importance and contribution of the above fragility model, which has already been employed in a seismic risk assessment in Portugal (Campos Costa et al. 2009), there are a number of reasons that may justify the development of a novel fragility/vulnerability model for Portugal: (i) the use of spectral ordinates for the inelastic period (thus a specific period for each level of ground motion) complicates the seismic risk methodology and does not allow the direct use of commonly available ground motion prediction equations (GMPE) to compute the ground motion at the location of the assets; (ii) the design parameters used in the construction of the capacity curve (strength coefficient, over-strength factor, elastic period and ductility factor) have been specifically calibrated for

structures typically found in the United States; (iii) the shape of the simplified capacity curve fails to account for the decrease in the base shear capacity due to P-delta effects; and, (iv) in the case of reinforced concrete building typologies, the influence of eventual masonry infill panels has been neglected.

Despite the availability of other fragility models developed for generic European buildings (Mouroux and Le Brun 2006), or for other countries whose building stock could have some similarities to the Portuguese one (e.g. Spain—Vargas et al. 2010, Italy—Borzi et al. 2008, Greece—Kappos et al. 2006), the characteristics in the structural capacity and response might not be realistically representative of Portuguese buildings, and consequently this could affect the reliability of the resulting earthquake loss estimation.

This paper hence focuses on the structural vulnerability of reinforced concrete buildings in Portugal, which represent about 50 % of the total building stock in the country, according to the 2011 Census Survey (http://censos.ine.pt/). Due to the lack of data regarding post-earthquake damage for this type of buildings in Portugal, an analytical methodology has been adopted herein. Thus, hundreds of models of moment resisting frames were produced to represent the RC building stock in Portugal, and subjected to one hundred ground motion records, using nonlinear dynamic analyses. In order to generate frames capable of reproducing the structural characteristics of the RC building stock in Portugal, 400 drawings were collected in many parts of the country, from public institutions, design offices and private practitioners, and subsequently analysed with the purpose of estimating the probabilistic distribution of a set of geometric parameters. Each generated frame was subjected to a nonlinear dynamic analysis per ground motion record, and two different criteria were employed to allocate each frame into a damage state. Several building typologies were considered herein, based on the date of construction (or seismic design philosophy and practice), number of storeys (or height of the structure) and seismic zonation, leading to 48 fragility models in terms of spectral acceleration. These results were combined with a consequence model (fraction of loss for each damage state), to produce a vulnerability model (set of loss ratios for a set of intensity measure levels), which can be used directly for economic loss estimation.

There are a number of limitations in the analysis carried out herein that need to be clarified. Each building is being represented by an isolated multi-degree of freedom system in a 2D environment, thus hindering the consideration of plan irregularities (which could result in torsional deformations) or pounding effects due to the existence of adjacent structures with significantly lower height. Moreover, levels below ground, inclined terrains and the possible existence of elements with a large stiffness, such as elevator shafts, shear walls or stairs cases were also neglected in this study.

These results were applied in a probabilistic seismic risk assessment for mainland Portugal, as described in Silva et al. (2014a).

1.1 Portuguese RC building stock

Reinforced concrete construction accounts for approximately 50 % of the Portuguese building stock and hosts 60 % of the national population, since on average it contains more dwellings than the other building typologies. Within this building class, at the time of the 2011 Census Survey, 49 % of the buildings had not been designed according to the most recent seismic code (RSA 1983), which represents approximately 3.1 million habitants living in structures that might not be capable of withstanding the effects on an eventual earthquake. Thus, the year of construction plays an important role in classifying the building portfolio according to the seismic design level.

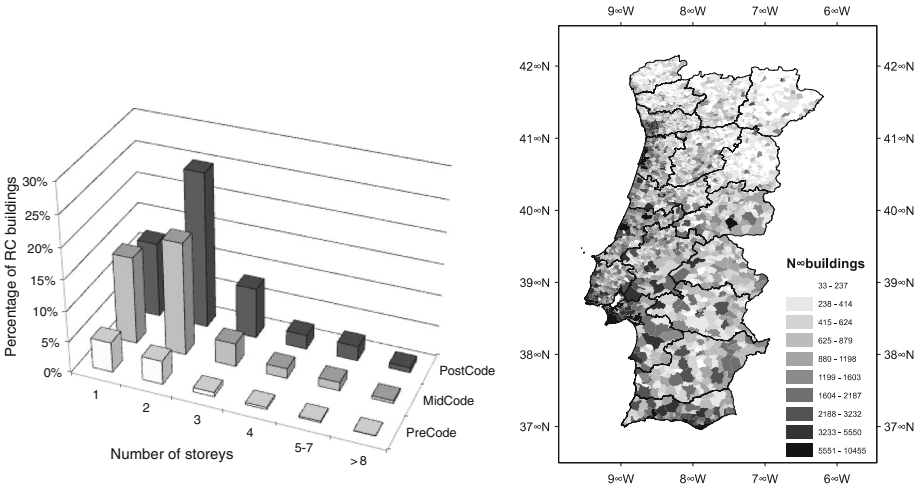

Fig. 1 Percentage of RC buildings according to year of construction and number of floors (*left*), and spatial distribution throughout Portugal at the parish level (*right*), according to the 2011 Census Survey

In Portugal, the first design codes that contained provisions regarding the consideration of seismic action date from RSCCS (1958) and RSEP (1961). In 1967, a regulation was introduced for reinforced concrete structures (REBA). However, such recommendations were overly simplified and did not impose adequate seismic performance requirements. Later, in 1983, a new and more demanding design code (RSA) was introduced, which is still in use nowadays, along with Eurocode 2—Design of Concrete Structures (CEN 2004) and Eurocode 8—Design of Structures for Earthquake Resistance (CEN 2005). In the present study, buildings that date before 1958 were categorized as pre-code (PC), whilst the buildings constructed between 1958 and 1983 were classified as mid-code (MC), and finally, the ones built after 1983 were termed as post-code (C). Within the latter two categories, it was also decided to consider a number of sub-categories according to the seismic zonation defined by the respective design codes. RSEP (mid-code) establishes three zones (A, B, C), whilst RSA defines four zones (A, B, C, D). Regarding the number of storeys, seven height categories were considered, following the same classes defined by the 2011 Census Survey: 1, 2, 3, 4, 5-7, >8 storeys. The combination between these three factors led to 48 RC building classes.

A summary of the RC building stock according to the design code and number of storeys, and their spatial distribution throughout mainland Portugal are illustrated in Fig. 1.

1.2 Geometric properties of Portuguese RC building stock

In this study, the material and geometric properties of the RC buildings with a moment-resisting frame as the principal structural system were thoroughly analysed. In order to do so, 200 drawings and design specifications from real buildings were gathered throughout the country, in cooperation with private practitioners, design offices and public institutions. The collection of blueprints from many parts of the country and from different entities was done with the purpose of capturing the variability in the structural design and construction practices endorsed in the different regions. Nevertheless, the set of blueprints that were considered were conditioned on the availability and willingness of the various private and public institutions to cooperate in this study.

An additional 200 drawings have been collected, but not considered for the study of the building characteristics, as they represented structures mainly composed of masonry or shear walls, vertically or horizontally very irregular or were related to industrial, public infrastructures or purely commercial buildings.

Ideally, a large sample of buildings from each category should be employed in the derivation of the statistics. However, considering a great number of buildings for each building class (in this study 48 classes have been defined) would lead to the analysis of thousands of drawings and design specifications, which evidently is impractical. Instead, a decision was made to group classes that shared similar trends. In order to evaluate this aspect, an analysis of variances—ANOVA (e.g. Wasserman 2004) was employed to understand whether or not the statistics of several groups were identical. This analysis revealed no significant differences in the geometry between buildings classified as pre-code and mid-code. A number of categories regarding the number of storeys were also created to evaluate the geometric parameters of the columns: low-rise: 1-3 storeys; mid-rise: 4-6 storeys; high-rise: > 7 storeys. Additionally, no distinction was done regarding the seismic zonation, as due to confidentially reasons the location of some of the buildings was unknown. Nevertheless, it is important to understand that during the generation of the RC frames used for the derivation of the fragility functions, the depth of the beams and columns was designed according to the seismic combination of loads established by each code, and thus the influence of the seismic zonation in the geometry is implicitly included. A similar study was carried out by Bal et al. (2008) for the characteristics of Turkish building stock and was used to guide the work undertaken and presented herein.

For each building drawing, the main frames in the structure that would resist lateral loads were chosen in order to measure the following set of geometric parameters: ground story and upper storeys heights, column widths and depths, beam lengths, widths and depths, and slab thicknesses. Then, the data for the various parameters was disaggregated according to the six building typologies, in order to assess if some geometric properties were directly related to the date of construction and/or number of storeys and hence they should be considered separately from the data of the other typologies.

The number of drawings analysed per building typology and its distribution per district in Portugal is presented in Fig. 2.

To model each geometric property, several probabilistic distributions (normal, lognormal, exponential, gamma, beta and weibull) were considered, and their statistical parameters derived using the maximum likelihood approach. Then, each distribution was evaluated in terms of the best-fit (i.e. the size of the residual between the reference and the modelled data) and goodness-of-fit (i.e. the capability of providing a satisfactory fit given a certain level of significance). For the latter, the Chi-square test was used for levels of 1, 5 and 10 % significance.

1.2.1 Inter-story height

RC buildings in Portugal frequently present differences in height between the ground story and the remaining upper floors (herein termed as the regular story height), usually due to the need to have wider spaces at the ground floor for commercial purposes or garages. The Portuguese legislation (RGEU 2007) has established since 1951 that a minimum clear height between the floor and the ceiling of 2.7 metres should be present in dwellings, and a minimum clear height of 3.0 metres is required in public areas, commercial spaces and offices. No significant differences were observed in the statistics when disaggregating the data according to date of construction or number of storeys and therefore, all of the data

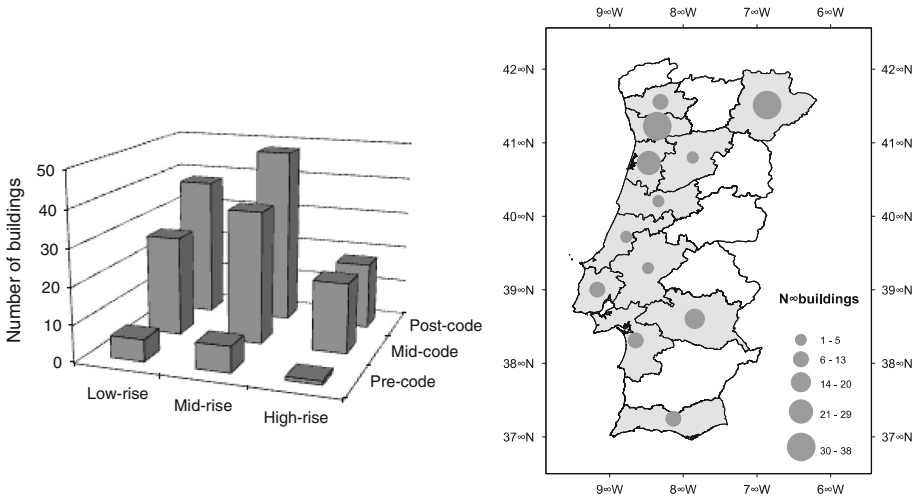

Fig. 2 Number of buildings analysed per number of storeys and date of construction (*left*) and the distribution per district in Portugal (*right*)

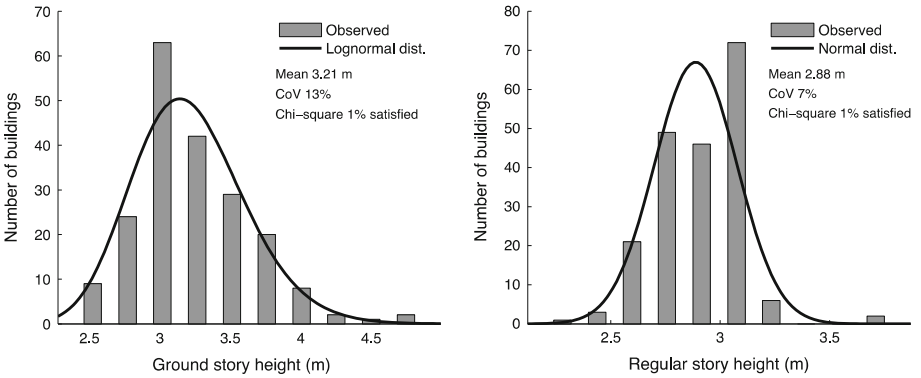

Fig. 3 Distribution of ground story (*left*) and regular story (*right*) heights for all RC buildings

was considered together in order to estimate these distributions. The ground story height was found to follow a lognormal distribution with a mean height of 3.21 metres and a coefficient of variation of 13 %, whilst the regular storey height was modelled with a normal distribution with a mean value of 2.88 metres and a coefficient of variation of 7 %. Both distributions proved to pass the Chi-square test with a significance level of 1 %. In Fig. 3, the histograms and associated probabilistic distributions of these parameters are illustrated.

The correlation between these two heights was estimated as 0.24, which can be considered insignificant. Thus, if the aforementioned statistics are used to generate synthetic frames, these two parameters can be sampled independently.

1.2.2 Column properties

For what concerns the column depth, the disaggregation of the data revealed a strong influence, as expected, in the number of storeys and time of construction. The dependence with

Table 1 Probabilistic distribution of column depth for each RC building typology

Building typology	Number of buildings	Probabilistic distribution	Mean (m)	Coefficient of variation (%)	A[a] (m)	B[a] (m)	Chi-square test (%)
Pre- and mid-code							
Low-rise	33	Lognormal	0.28	15	0.20	0.44	NS[b]
Mid-rise	43	Normal	0.36	23	0.24	0.55	10
High-rise	20	Lognormal	0.57	40	0.28	1.00	10
Post-code							
Low-rise	38	Normal	0.38	20	0.26	0.60	10
Mid-rise	48	Lognormal	0.43	20	0.28	0.70	5
High-rise	18	Lognormal	0.51	36	0.30	0.95	10

[a] A and B represent the minimum and maximum values of the observed data respectively
[b] NS signifies that the Chi-square test could not be satisfied for any of the established significance levels

the building height is certainly due to the higher axial loads in taller buildings, which consequently leads to columns with larger sections. Regarding the time of construction, the increase in the column depth and width is probably due to the implementation of the seismic code of 1983, imposing higher bending moments in the design process, thus leading to longer sections, as was also verified in the depth of the beams. The statistics for the column depth are summarized in Table 1.

With regards to the column width, a slightly different behaviour was observed. For the pre-code buildings, no relevant discrepancies were verified in the column width between buildings with a distinct number of storeys. In fact, during the process of evaluating the drawings, it was noticed that the majority of the columns from the pre-code buildings were only designed to withstand the bending moment in a single direction. Therefore, the column width was frequently established a priori within a range between 0.20 and 0.30 metres, as it was assumed that these elements would not have to resist any significant bending moment in this direction. Concerning the column width for the post-code buildings, the implementation of the 1983 seismic code, the introduction of automatic tools and the three-dimensional design of the structures propelled the consideration of larger bending moments in the two directions, leading to columns with increasing sections (not just a greater depth but also width as discussed before) with the number of storeys. The results for this parameter are described in Table 2.

1.2.3 Beam properties

As previously mentioned, for each drawing only the frames that provided the main lateral load resistance to the building were considered. This approach allowed the elements that were built mainly for aesthetics or to support secondary elements (e.g. balconies) to be neglected. The investigation of the beam properties covered the beam length, width and depth.

Regarding the first two parameters, no significant differences in the statistics were observed when disaggregating the data based on the date of construction or number of storeys, probably due to the fact that the beam length is more influenced by architectural requirements and the beam width is related with the thickness of the walls and depth of the beams, rather than code guidelines or the height of the building. Beam length was found to have a mean of 4.37 metres with a coefficient of variation of 11 %, while for the beam width a mean of 0.27 metres with

Table 2 Probabilistic distribution of column width for each RC building typology

Building typology	Number of buildings	Probabilistic distribution	Mean (m)	Coefficient of variation (%)	A[a] (m)	B[a] (m)	Chi-square test (%)
Pre- and mid-code	96	Lognormal	0.27	16	0.20	0.53	NS[b]
Low-rise	38	Normal	0.25	11	0.20	0.30	1
Post-code							
Mid-rise	48	Normal	0.27	13	0.20	0.37	1
High-rise	18	Lognormal	0.31	23	0.21	0.53	NS[b]

[a] A and B represent the minimum and maximum values of the observed data respectively
[b] NS signifies that the Chi-square test could not be satisfied for any of the established significance levels

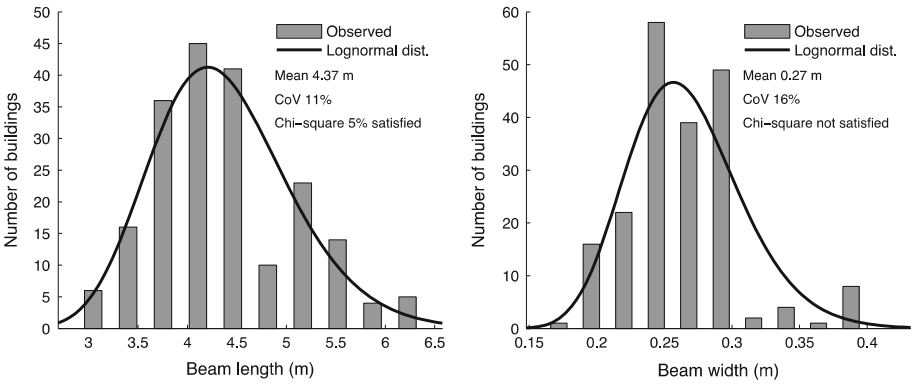

Fig. 4 Distribution of beam length (*left*) and width (*right*) for all RC buildings

a coefficient of variation of 16 % was calculated. Both geometric parameters were modelled using a lognormal distribution, but the former satisfied the Chi-square test for a significance level of 5 % whilst the latter did not satisfy this test for any of the established significance levels. The results for these parameters are presented in Fig. 4.

For the beam depth, a relevant discrepancy was observed in the statistics between the buildings constructed before and after the implementation of the design code of 1983. Thus, the data has been separated and the beam depth for the pre-code was assumed to follow a normal distribution with a mean of 0.44 metres and associated coefficient of variation of 22 %, whilst for the post-code buildings a lognormal distribution was used with a mean of 0.50 metres and coefficient of variation of 18 %. For the pre-code beam depth, it was possible to satisfy the Chi-square test for a significance level of 1 %, though for the post-code beam depth, in which despite the low residual between the observed data and the probabilistic model, none of the significance levels were respected. Figure 5 presents the results for this geometric parameter.

A clear increase in the beam depth can be seen between the pre- and post-code buildings, probably due to the fact that the adequate consideration of the lateral loads due to the seismic action led to higher bending moments in the beams, and consequently a greater depth to withstand such demands.

Moreover, the correlation between the beam geometric parameters has been investigated, as the calculation of beam depth should be directly related to the beam length. For the pre-

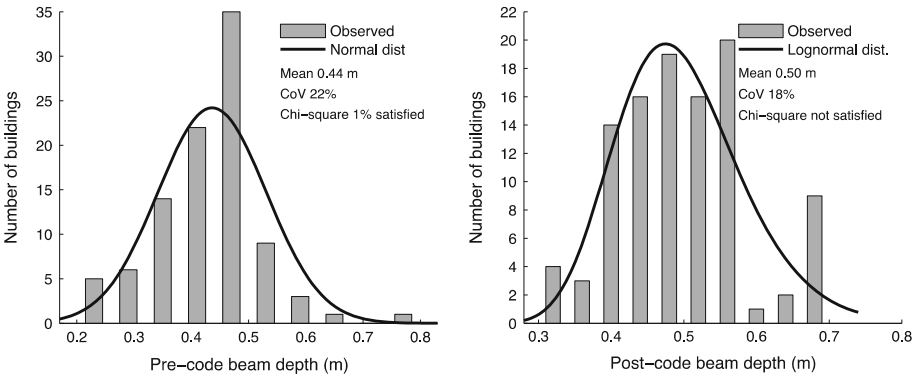

Fig. 5 Distribution of beam depth for pre- and mid-code (*left*) and post-code (*right*) RC buildings

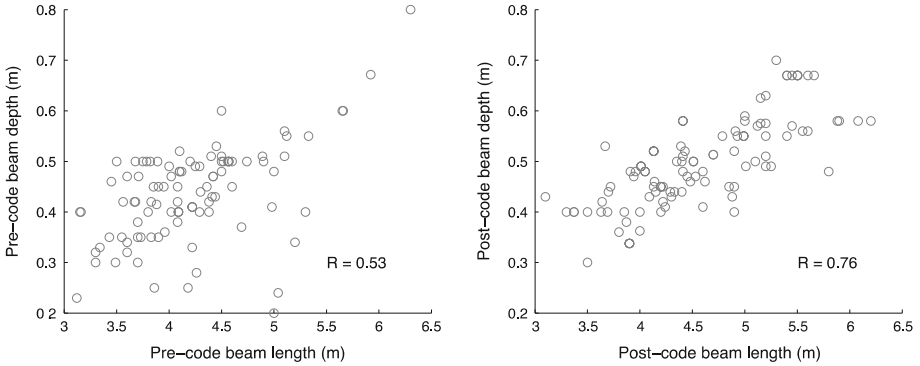

Fig. 6 Correlation between beam length and depth for pre/mid-code (*left*) and post-code (*right*) RC buildings

code buildings, a correlation of 0.53 was estimated while for the post-code buildings, a larger correlation of 0.76 was observed. This increase in the correlation for the post-code buildings might be due to the introduction of automatic tools in the design of the buildings, leading to section dimensions uniquely calculated for each structural element. In fact, during the process of evaluating the drawings and design specifications, it was observed that buildings with similar dimensions but with distinct construction times had a striking difference in the variability of the structural elements dimensions. Buildings built more recently were frequently designed with tens of different beams whilst for the pre-code buildings, only a few sections were designed and applied repeatedly in beams often with different lengths. The employment of the correlation factor during the generation of synthetic RC building frames using a Monte Carlo sampling approach is fundamental to ensure that unrealistic structural elements are not created (e.g. long beams with very small section depth). The scatter between the beam depths and the respective beam lengths are depicted in Fig. 6.

1.2.4 Slab thickness

The floors of the common RC buildings in Portugal are mostly composed of pre-cast pre-stressed RC beams with clay hollow blocks and a cast-in-place concrete topping layer, and this is mainly found in the central and northern part of Portugal. It is also possible to find purely

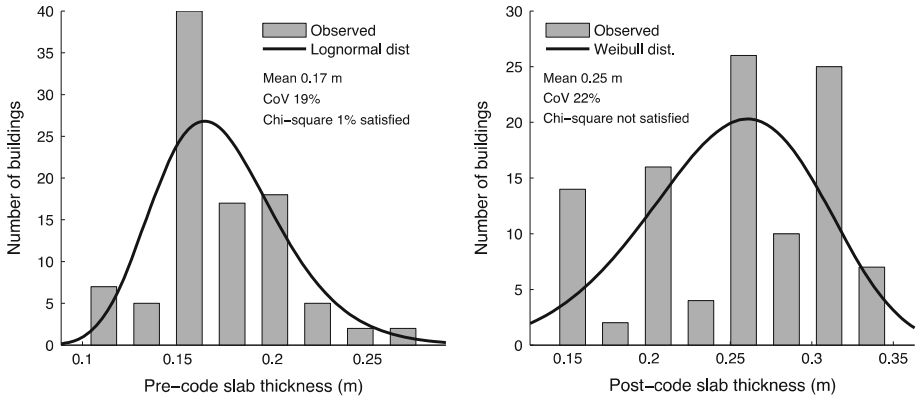

Fig. 7 Distribution of slab thickness for pre- and mid-code (*left*) and post-code (*right*) RC buildings

cast-in-place reinforced concrete slabs, mainly in floors with long spans or more recently, in flat slab buildings only consisting of columns and slabs, without the use of beams. This structural configuration is frequently found in large cities such as Lisbon. The thickness of the slabs was also investigated, as it is an important parameter to be considered in the estimation of the gravity loads. Again, the data was disaggregated based on the date of construction (pre- and post-code), and the respective results are illustrated in Fig. 7.

1.3 Material properties of Portuguese RC building stock

An attempt has also been made herein to investigate the probabilistic distribution of the concrete and steel mechanical properties of Portuguese buildings. In order to estimate such statistics, ideally a large number of random buildings should be selected, and field tests should be carried out to calculate properties such as the concrete compressive strength and steel rebar yielding and ultimate strength. Since such endeavour would require a great amount of human and economic resources, for the concrete compressive strength, it was decided to take advantage of the availability of data from measurements on buildings that were subjected to structural retrofitting/rehabilitation or demolition, provided by public and private institutions that carried out those tests on the concrete. The measurements were mostly done through destructive approaches, in which a concrete drilling core was extracted from a column or beam, and compressed until rupture in the laboratory. For the steel properties, the results from previous studies have been investigated and employed.

1.3.1 Concrete properties

Regarding the code specifications for concrete properties, the first regulation that imposed minimum requirements for the compressive strength dates from 1918 (120 kg/cm^2 or ≈12 MPa), which was later replaced by another regulation in RBA (1935) (180kg/cm^2 or ≈18 MPa). These thresholds were established for the mean concrete compressive strength (f_{cm}), which had the disadvantage of allowing the possibility of using concrete with considerably lower resistance. Hence, in 1967 the regulation was changed (REBA) enforcing the use of the characteristic compressive strength (f_{ck}), a minimum resistance value that features a 95 % probability of being exceeded. This regulation also introduced the concept of classes of concrete resistance, each one with a characteristic compressive strength, varying from

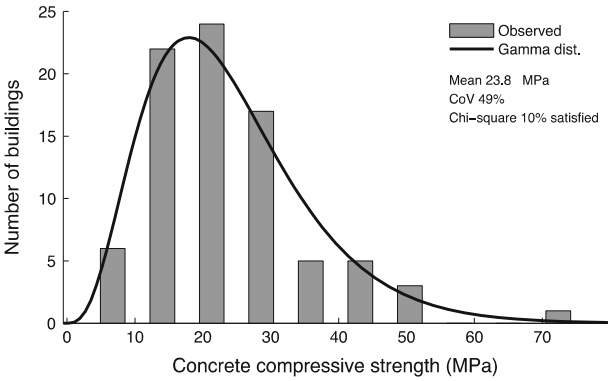

Fig. 8 Concrete compressive strength distribution

approximately 18 to 40 MPa. Finally, in the 1983 regulation (RSA), and in the more recently proposed Eurocode 2 (CEN 2004), the concrete classes were adjusted to the international units (MPa) and extended to a compressive strength of 55 MPa.

To derive the concrete compressive strength statistics, the experimental results from core drilling tests in 76 buildings located mainly in the centre and north of Portugal were employed. Unfortunately, it was not possible to disaggregate this data based on the date of construction or resistance class, since privacy restrictions prevented access to such complementary information. A gamma distribution seemed to provide the best fit with a mean value of 23.8 MPa and a coefficient of variation of 49 % (leading to a characteristic compressive strength of 8 MPa), as depicted in Fig. 8.

The scatter of the results is characterized by a large coefficient of variation, probably due to the fact that the samples were taken from buildings constructed in different time periods, meaning that the structures were designed considering different resistance classes and different design codes. In fact, Almunia (1993) suggested a significantly lower coefficient of variation (between 6 and 11 %) for the variability of the concrete compressive strength within the same resistance class. These levels of variability are clearly more adequate to employ in the derivation of fragility models, and a similar effort should be carried out for the building typologies in Portugal. Nevertheless, in the work of Bal et al. (2008), in which a similar process was employed to estimate the probabilistic distribution of this parameter, a similar coefficient of variation to the one found herein was obtained (51 %).

1.3.2 Steel properties

The development of the code specifications regarding the steel properties followed an evolution similar to that described previously for the concrete. The first regulations date from 1918 and 1935, and required an ultimate tensile strength greater than 3800 kg/m^2 (≈387 MPa) and 3700 kg/m^2 (≈377 MPa) for reinforced plain steel bars, respectively. By the end of the 1940s, high resistance steel was introduced in Portugal and in order to fully explore this higher level of resistance, the interaction between concrete and steel was enhanced by the application of ribs on the bars, which are now mandatory according to design codes (Pipa 1993). In the 1967 code (REBA), steel resistance classes (A24, A40, A50) were adopted, each class defined by a characteristic yielding tensile strength (f_{yk}). Later in the 1983 regulation

Table 3 Probabilistic distribution of steel yielding strength (produced in Portugal) proposed by Pipa (1993)

Steel class	Size of sample	Mean yielding strength (f_{ym}) —(MPa)	Standard deviation of yielding strength (σ_y)—(MPa)	Coefficient of variation (%)
A400	84	495	22	4.4
A500	51	589	30	5.1

(RSA) and in the Eurocode 2 (CEN 2004), these classes were modified to A230/A400/A500 and S400/S500/S600, respectively.

In Portugal, the majority of the buildings have been designed using steel ribbed bars with a nominal strength of 400 and 500 MPa, and a smaller fraction with plain bars with a lower resistance, mainly in reinforced concrete buildings constructed until the 1970s. In the work of Pipa (1993), several material parameters (yielding and ultimate strength and strain) of A400 and A500 steel classes were analysed using experimental results from a sample with about 700 specimens, coming from many European producers (e.g. Italy, Portugal, Spain, United Kingdom). Each parameter was assumed to follow a normal distribution and a mean and standard deviation was computed for the complete sample. More specifically for the steel yielding strength, its probabilistic distribution was estimated considering only the steel bars produced in Portugal. The latter statistics are presented in Table 3, and will be used in the development of the vulnerability model for the reinforced concrete moment-resisting frame building stock in Portugal.

The variability in the steel material properties is usually fairly constrained, due to the industrialized process used in its production that can be well controlled. Its effective yielding strength is considerably higher than the nominal strength, probably due to the safety factors considered in its production process. In the work of Fernandes et al. (2011), Rodrigues et al. (2012), Lopes (2012) and Melo et al. (2012), the yielding strength of a smaller sample of steel bars was estimated, and results within the range proposed by Pipa (1993) were obtained.

From the evaluation of the technical specifications from the sample of RC buildings constructed after the 1983 regulation, both steel classes seemed to be used with the same frequency. Hence, both types of steel were used with equal weight in the development of the vulnerability model herein. For buildings prior to this code, the employment of steel of class A230 (or A24) was also found. A comprehensive statistical study regarding the material properties of this class of steel for Portugal does not currently seem to exist. For this reason, the mean yielding strength of 344.3 MPa for European and Mediterranean buildings proposed in Carvalho and Coelho (2001) was adopted. Regarding the uncertainty in this parameter, a coefficient of variations of 5 % was assumed, which is in agreement with the previously described results for modern steel.

The development of the vulnerability functions for buildings constructed prior to the 1983 regulation, a steel of class A400 was used with a relative weight of 0.5 and steel of classes A500 and A230 were used with equal weights of 0.25 each.

2 Development of the vulnerability model

In this section, an analytical methodology that uses nonlinear dynamic analysis to calculate a fragility model (i.e. a collection of curves describing the probability of exceeding a number of

limit states for a set of intensity measure levels) is described. Then, these results are converted into a vulnerability model (i.e. mean loss ratio and associated coefficient of variation for a set of intensity measure levels) through the employment of a consequence model (i.e. the ratio between repair cost and replacement cost for each damage state). When applying such approach to derive a set of vulnerability functions, there are four main aspects that strongly affect the results: (i) the structural modelling of the building typologies; (ii) the damage state criteria; (iii) the selection of the ground motion records; and (iv) the consequence model employed to convert fragility curves into vulnerability curves. The various assumptions and main results from each of the aforementioned components are further discussed in what follows.

2.1 Structural modelling of the RC frames

The geometric and material probabilistic distributions presented in the previous section have been used to randomly generate one hundred assets for each building typology. Then, the percentage of flexural reinforcement in each structural element is estimated taking into account the code level of the building typology within which the building falls: (i) pre-code (before the 1958 code)—designed only for gravity loads; (ii) mid-code (between 1958 and 1983 codes)—designed for both gravity and seismic action according to simplified considerations in the definition of the latter; and (iii) post-code (after the 1983 code)—designed for gravity and lateral loads, which were calculated based on the uniform hazard spectra for both types of seismicity (short distance with moderate magnitude and far distance with large magnitude, whichever led to a greater ground shaking) in very hard soils (Vs30 $>$ 360 m/s), which are the most common soil type in Portugal (Silva et al. 2014a).

To keep the computational effort at a reasonable level, each asset is represented by a 2D frame with 3 bays. This approach has the advantage of allowing the consideration of the uncertainties in the capacity, rather than using a single structure believed to be representative of a given building typology. Each frame was modelled using a 2D structural analysis environment, thus considering only 3 degrees of freedom per node (2 translations and 1 rotation) and all the columns and beams were modelled as force-based fibre elements with five integration points. The cross-sections were discretized in fibres in order to capture the nonlinear behaviour of the materials, with a mesh of 5×50 fibres. The unconfined and confined concrete constitutive relationships were assumed to follow the Kent-Park model modified by Scott et al. (1982) with a confinement coefficient equal to 1.15, whereas the behaviour of the steel was represented by the model suggested by Giuffrè and Pinto (1970). The gravity loads were applied in the structure as distributed uniform loads on the beams, and P-delta effects were considered.

The infill panels were modelled with two diagonal compression struts, which is a common approach adopted in some guidelines (FEMA273 1997; NZSEE 2006). Such model has the disadvantage of neglecting the interaction between the two diagonal elements (Rodrigues et al. 2010) or the local shear forces introduced by the panel near the column ends (Smyrou 2006). However, given the large sample of assets and the wide spectrum of variables considered in this study, it was concluded that this improvement in the model was not worth the significant increase in the complexity of the analyses. The force-displacement model used to represent the strut's nonlinear response is depicted in Fig. 9.

Several other relationships for the force-displacement model can be found in the literature (e.g. FEMA273 1997; Hashemi and Mosalam 2007; Dolšek and Fajfar 2008; Rodrigues et al. 2010). Nevertheless, the majority of the models are comprised by an initial branch with a linear behaviour, followed by a reduction in stiffness due to the formation of cracks in

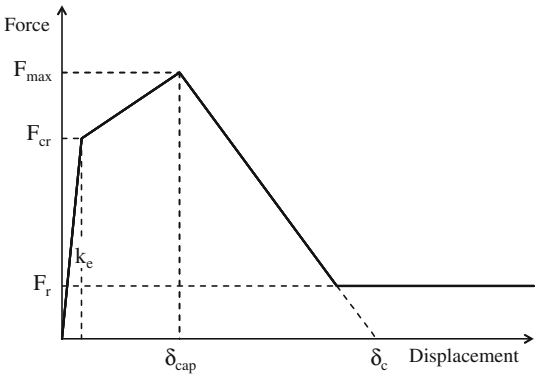

Fig. 9 Idealized force-displacement relationship for each infill strut (adapted from Sattar and Liel 2010)

the infill panel, a short plateau due to the low ductility characteristic of masonry walls, and ending with an abrupt loss in strength capacity due to shear or crushing failure. Some models also consider some residual strength, such as the one adopted herein.

The equivalent strut width (w_{inf}) was computed considering the proposal from Stafford-Smith and Carter (1969), which uses the following formula:

$$w_{inf} = 0.58 \left(\frac{L_{inf}}{h_{inf}}\right)^{-0.445} (\lambda_i h_{col})^{0.335} r_{inf} \left(\frac{L_{inf}}{h_{inf}}\right)^{0.064} \quad (1)$$

where h_{col} stands for the column height and L_{inf}, h_{inf} and r_{inf} represent the length, height and diagonal length of the infill, respectively. The λ_i stands for a non-dimensional parameter expressing the relative stiffness of the frame to the infill and can be calculated through the following formula:

$$\lambda_i h_{col} = \left(\frac{E_{inf} t_{inf} sin\,(2\theta)}{4 E_f I_{col} h_{inf}}\right)^{0.25} \quad (2)$$

where E_{inf} and t_{inf} represent the elasticity modulus and the thickness of the infill panel, respectively; E_f stands for the elasticity modulus of the frame; θ is the angle between the diagonal of the infill and the horizontal; and I_{col} refers to the moment of inertia of the columns.

The initial stiffness (k_e) was computed as suggested by Sattar and Liel (2010) with the formula:

$$k_e = 2 \left(\frac{E_{inf} w_{inf} t_{inf}}{r_{inf}}\right) \cos(2\theta)^2 \quad (3)$$

The formula proposed by Dolsek and Fajfar (2008) was used to compute the maximum force (F_{max}), the cracking force of the infill (F_{cr}) was assumed as 55 % of the latter, the deformation at maximum force (δ_{cap}) was assumed as 0.10 % (for panels with openings) or 0.20 % (for panels without openings) and the deformation at zero wall strength (δ_c) was established as 5 times the latter deformation (Dolšek and Fajfar 2008; Sattar and Liel 2010; Uva et al. 2012). The strength and the initial stiffness in panels with openings were reduced by a factor λ_0, according to the work of Dawe and Seah (1988):

$$\lambda_0 = 1 - \frac{1.5 L_{op}}{L_{inf}} \quad (4)$$

where L_{op} represents the horizontal length of the opening. The consideration of openings in the infill panels allows for a more realistic modelling of the frame, rather than considering it bare or fully infilled. In our study, in order to keep a fair balance between the different types

of panels, it was decided to consider one bay as fully infilled, one bay with large openings (i.e. doors) and another bay with small openings (i.e. windows). Their position was randomly allocated within the floor. Regarding the ground floor, some frames were modelled with three panels with large openings at this level, in order to take into account the portion of buildings with open-space configurations for commercial purposes (10 % based on information from the Building Census survey of 2011).

The characteristics of the masonry infills have been established based on the findings of Vicente (2004) and Soares (2012), as well as through expert opinion.

2.2 Damage state definition criteria

The possible options for the limit state criterion can vary significantly and a recognized common approach regarding which criteria should be employed for the development of fragility functions does not seem to exist. As discussed by Akkar et al. (2005) and Erberik (2008), the employment of a local criterion (e.g. member deformation, hinge mechanisms or concrete/steel strains) to define the limit states when generating fragility curves for population of buildings may not be appropriate. Hence, a global parameter such as maximum global drift (e.g. Akkar et al. 2005; Silva et al. 2014b) or maximum interstory drift (e.g. Hancilar et al. 2006; Rossetto and Elnashai 2005) was preferred in this study. Both of these parameters have been independently considered herein.

2.2.1 Maximum global drift

For the estimation of the global drift limits, a displacement-based adaptive pushover curve (Antoniou and Pinho 2004) was derived for each frame without the masonry infills (bare frame), and four limit state global drifts were extracted based on the following criteria:

- Slight damage: global drift when 50 % of the maximum base shear capacity is achieved;
- Moderate damage: global drift when 75 % of the maximum base shear capacity is achieved;
- Extensive damage: global drift when the maximum base shear capacity is achieved;
- Collapse: global drift when the base shear capacity decreases by 20 % or 75 % of the ultimate global drift taken from the pushover curve, whichever is achieved first.

Similar thresholds for the global drift limits have been used by various authors (e.g. Erberik 2007; Papaila 2011). The consideration of the infill panels in the numerical models causes a significant decrease in the displacement capacity. In order to take into account this aspect, the reduction parameters proposed by Bal et al. (2010) for each limit state were employed. The latter study suggests a factor of 0.52 for the displacement until the yielding point (moderate damage), a factor of 0.40 for the displacement between the yielding point and the third limit state (extensive damage) and a factor of 0.28 for the displacement between the same point and the fourth limit state (collapse). This reduction due to the influence of the infill panels is depicted in Fig. 10.

2.2.2 Maximum inter-story drift

For the estimation of the inter-story drift limits, Kirçil and Polat (2006) demonstrated a procedure to estimate the inter-story drift for yielding and collapse limit states by employing Incremental Dynamic Analysis (IDA—Vamvatsikos and Cornell 2002) in single structures. However, applying such an approach would soon become impractical due to the large sample

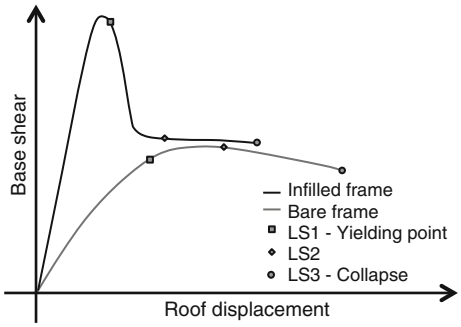

Fig. 10 Reduction in the displacement capacity between bare and infilled frames (adapted from Bal et al. 2010)

Table 4 Limit state inter-story drifts for infilled MRF proposed by Rossetto and Elnashai (2003)

Damage state	Inter-story drift (%)
Slight	0.05
Light	0.08
Moderate	0.3
Extensive	1.15
Partial collapse	2.8
Collapse	>4.4

of structures considered herein. As an alternative, instead of computing these values for each structure, a fixed set of inter-story drifts (one per limit state) proposed by Rossetto and Elnashai (2003) was applied to the complete sample. In the latter study, the authors evaluated the progression of the global damage with increasing inter-story drift in 25 dynamic tests for RC moment resisting frames (MRF) and the maximum inter-story drift was estimated for six limit states, as described in Table 4.

In order to adapt this damage scale (six levels), to the one previously adopted for the global drift parameter (four levels), the light and slight damage states were merged as one (since both are related only to non-structural damage) with an inter-story drift threshold of 0.05 %. Partial collapse and collapse were equally merged, becoming a single damage state with an inter-story drift limit of 2.8 %.

Clearly, both global parameters have strengths and limitations. Inter-story drift tends to provide a better correlation with damage, but it is not easily assessed for each structure and thus often a fixed set of limit state values are used, regardless of the structural properties. On the other hand, the global drift for each limit state can be derived taking into account the structural characteristics of each frame at a low computational effort. However, in frames where a soft-story failure mechanism might develop or in vertically irregular structures in which the maximum lateral displacement might occur at intermediate floors, this global parameter could fail to establish the level of damage. For these reasons and to comprehend how the damage state criteria might affect the resulting limit state curves, fragility models were developed separately using each global parameter criterion.

2.2.3 Residual inter-story drift

Residual inter-story drifts were also evaluated, as buildings with permanent large displacements are often likely to be demolished. The probability of demolition is related with the level of residual drift sustained by the building after the earthquake. Ramirez and Miranda (2012)

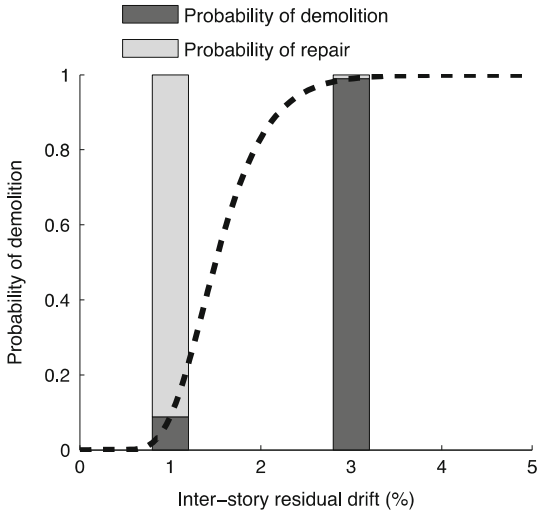

Fig. 11 Probability of demolition as a function of the inter-story residual drift

proposed to model the demolition probability using a cumulative lognormal distribution with a median of 1.5 % and a logarithmic standard deviation of 0.3 %. Such statistics were derived based on a limited number of post-earthquake cases, as well as expert judgement. Following this distribution, a building with a residual inter-story drift of 1 % would lead to a probability of demolition of 10 %, whilst a building with a residual drift of 3 % would be almost certainly (99 %) demolished. This process is clarified in Fig. 11.

Hence, a building sustaining moderate or extensive damage might actually represent a greater loss, due to the necessity for its demolition and full replacement. This aspect might not be relevant in the development of a fragility model, whose main purpose is to simply provide the distribution of buildings in a number of damage states for a set of intensity measure levels, but it is certainly fundamental in the development of a vulnerability model, which should be capable of providing percentages of economic loss for various levels of seismic intensity. For this reason, in the calculation of the vulnerability functions, a second fragility model was developed in which after each nonlinear dynamic analysis, if the RC frame presented considerable residual inter-story drifts, the probabilistic distribution proposed by Ramirez and Miranda (2012) was used to assess whether the frame should be placed in the collapse damage state, or remain in the one indicated by the global damage criteria.

2.3 Selection of ground motion records

For what concerns the selection of a set of ground motion records to carry out the nonlinear dynamic analyses, Portugal represents a challenging case as only three seismic events with significant ground motion were ever recorded. For this reason, records from other regions in the world with similar geological and tectonic characteristics (e.g.: Spain, France, Switzerland, Northwest Africa, Central and Eastern North America) were gathered. For further information regarding the Portuguese tectonic environment, readers are referred to Vilanova and Fonseca (2007).

In order to understand which earthquake magnitude and distance intervals contribute most to the hazard in Portugal, the hazard disaggregation carried out by Peláez Montilla et al. (2002) and Sousa and Costa (2009) was used. Despite the different conclusions between these studies,

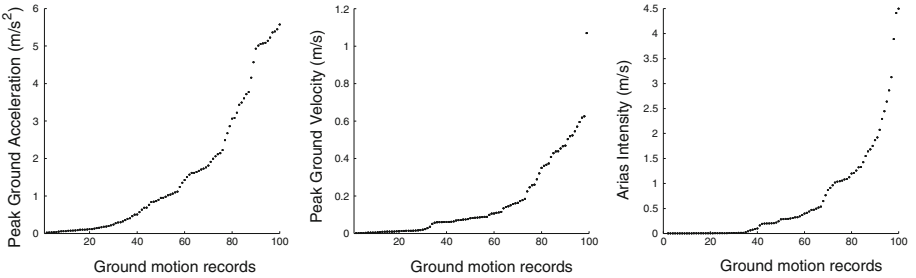

Fig. 12 Distribution of the PGA (*left*), PGV (*centre*) and Arias Intensity (*right*) in the selected records

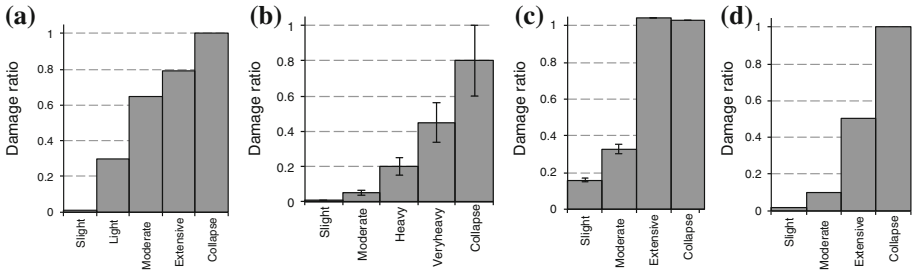

Fig. 13 Consequence models for **a** Italy (Di Pasquale and Goretti 2001); **b** Greece (Kappos et al. 2006); **c** Turkey (Bal et al. 2008) and **d** California (FEMA-443 2003)

it is fair to state that significant ground motion in Portugal is mainly produced by shallow earthquakes with low to moderate magnitude (4.5–6.5 Mw) at short distances (10–80 km) generated in stable continental regions (SCR) and deep earthquakes with moderate to large magnitudes (6.5–8.0 Mw) at long distances (100–200 km) generated in active shallow crustal regions (ASCR). These combinations of magnitude/distances were respected in the selection of the accelerograms to ensure a sample of records compatible with the seismicity in Portugal. One hundred ground motion records were extracted from the PEER (http://peer.berkeley.edu/smcat/), ESD (http://www.isesd.hi.is/), RAP (http://www-rap.obs.ujf-grenoble.fr/) and SED (http://seispc2.ethz.ch/strong_motion/home.jsp) databases, and the variation of PGA, PGV and Arias Intensity of these records is presented in Fig. 12.

2.4 Evaluation of consequence models

Consequence models can be used to convert a set of fragility functions (probability of exceeding a set of limit states versus a set of intensity measure levels) into a vulnerability function (mean loss ratio and corresponding coefficient of variation versus a set of intensity measure levels). A model describing the distribution of cost ratio (also known as damage ratio, providing the ratio of cost of repair to cost of replacement) for a set of damage states does not seem to currently exist for Portugal. Such models are commonly derived based on information regarding the repair costs claimed by householders after the occurrence of an earthquake, which hampers the development of consequence models for countries such as Portugal, where earthquakes are not frequent. For this reason, consequence models developed for other regions (Italy, Greece, Turkey and California) were considered, (see Fig. 13).

These models present different damage scales and hence each damage ratio might be influenced not just by the level of damage in the structure, but also by local policy; for exam-

Table 5 Consequence model used in the development of the vulnerability model for the Portuguese RC building stock

Damage state	Damage ratio	
	Mean	Coefficient of variation
Slight	0.1	30
Moderate	0.3	20
Extensive	0.6	10
Collapse	1.0	0

ple, Turkish law states that a building sustaining extensive damage should not be repaired, and must be demolished instead. The aforementioned four models were used to estimate a consequence model to be used in the development of the vulnerability functions for the Portuguese RC building stock. To do so, an average between the cost ratios of the damage states equivalent to those considered in this work was estimated. The damage ratio for extensive damage in the Turkish model was neglected, as the criteria behind this value (i.e. that buildings falling in this damage state need to be demolished and replaced) is not valid for Portugal.

Consequence models are potentially one of the main sources of uncertainty in the derivation of vulnerability models, as the fraction of loss for a given damage state may vary greatly. Besides the work of Bal et al. (2008) in which a coefficient of variation of damage ratio for moderate damage is indicated, other quantitative studies about this level of uncertainty do not seem to exist. Therefore, in order to somehow incorporate this uncertainty in the vulnerability function calculations, a coefficient of variation in the damage ratio distribution for each damage state was established based on the statistics presented by Bal et al. (2008), the ranges proposed by Kappos et al. (2006), as well as expert judgement. A beta distribution was adopted to constrain the damage ratios between 0 and 1. The resulting distributions used in this present study are described in Table 5.

2.5 Fragility methodology

For the purposes of deriving a set of fragility functions for each RC building typology, a framework was developed in Matlab (http://www.mathworks.com/) to handle the various inputs/outputs, to generate the RC frames and to perform the final statistical regressions. This framework was connected to OpenSEES (http://opensees.berkeley.edu/), an open source software for structural analysis, to derive the pushover curves and to carry out the nonlinear dynamic analysis. The overall process can be summarized in the following steps:

1. Random generation of a population of RC frames through Monte Carlo simulation, considering the material and geometric variability, code level and distribution of buildings regarding the number of storeys within each building typology;
2. Computation of a displacement-based adaptive pushover curve for each frame, with the purpose of estimating a set of limit state global drifts;
3. Perform nonlinear dynamic analyses for each RC frame using a large selection of ground motion records, with the purpose of extracting the maximum global and inter-story drifts;
4. Allocate each RC frame into a damage state based on the global (step 2) or inter-story drift criteria and verify if collapse was achieved due to excessive residual inter-story drift;
5. Calculate the cumulative percentage of buildings for each limit state versus the representative intensity measure of each accelerogram (e.g.: $Sa(T_{el})$, PGA);

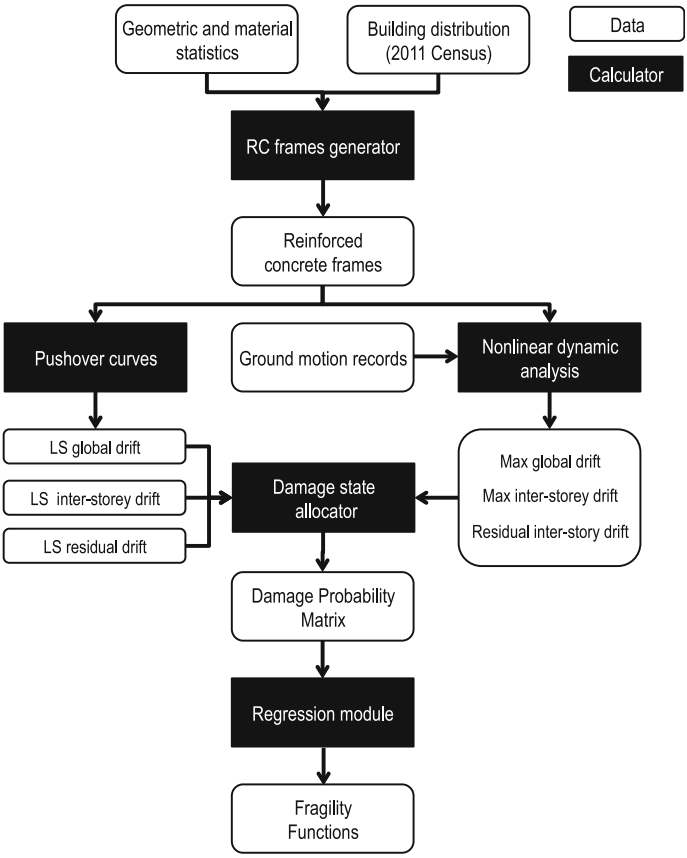

Fig. 14 Analytical fragility methodology workflow

6. Carry out regression analysis to calculate the parameters (mean and standard deviation) of the fragility functions (assumed to follow a lognormal distribution).

This process is schematically illustrated in Fig. 14.

3 Results

3.1 Evaluation of the RC frames

3.1.1 Elastic period of vibration

When employing an analytical methodology to derive a vulnerability model, in which Monte Carlo sampling is used to create a synthetic collections of assets, it is important to verify whether the structures that are being generated are reasonable and in agreement with the real characteristics of the building stock. To carry out this verification, various structural and dynamic parameters were estimated, and compared with results from previous studies and experimental campaigns. The first verification was done in terms of the elastic period (first

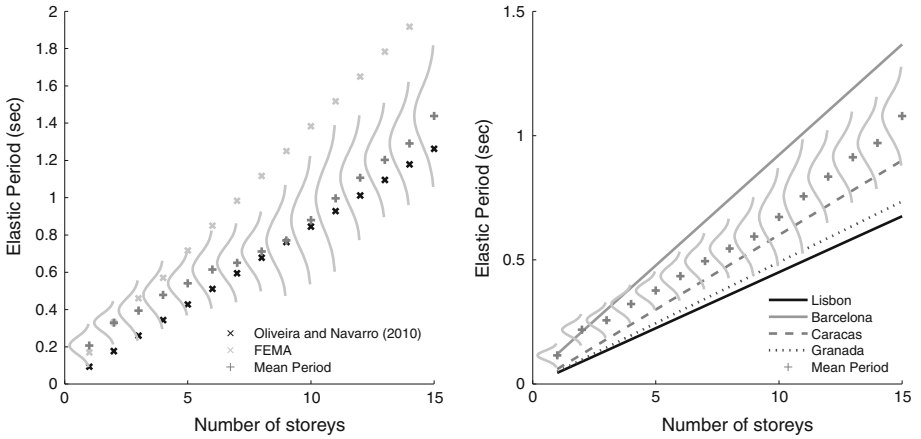

Fig. 15 Comparison between the elastic periods for the bare frames computed herein and FEMA (1999) (*left*) and between the elastic period for infilled frames computed herein and previous studies (*right*)

mode) of the frames with and without infill panels. For the former comparison, empirical relationships between the main period of vibration and building height were used, as proposed by Oliveira and Navarro (2010), according to in-situ dynamic measurements performed for Portuguese reinforced concrete frame structures. For the latter, a set of empirical formulae providing the elastic period as a function of the number of floors was employed. These equations were derived based on field measurements of the period of vibration of tens of real RC buildings with infill walls in Barcelona, Spain (Espinoza 1999); Caracas, Venezuela (Enomoto et al. 2000); Granada, Spain (Kobayashi et al. 1996) and Lisbon, Portugal (Navarro and Oliveira 2004). One hundred pre-, mid- and post-code representative frames were randomly generated for each combination of design epoch and number of storeys, and the mean period and respective probability density function are presented in Fig. 15, along with the results from the aforementioned studies.

For what concerns the bare frames period of vibration, the estimated trend is relatively similar to the analogous results arising from the prediction for typical Portuguese buildings, considered as the mean between longitudinal and transversal estimates derived by Oliveira and Navarro (2010), as a function of number of floors. For what concerns the comparison with the FEMA formulae, the results attained herein are considerably lower. As indicated by Oliveira and Navarro (2010), the FEMA methodology employed by Carvalho et al. (2002) has been developed for buildings in the United States, whose geometric characteristics tend to impart a more flexible behaviour, and consequently, a longer period, as verified by the findings of this study.

Regarding the evaluation of the periods of infilled frames, slight overestimation was observed for the empirical relationships with results within the range established by the cases of Lisbon and Granada. To this end, empirical relationships for buildings in other cities (e.g. Almeria, Spain; Grenoble, France; Potenza, Italy), whose results are in agreement with the aforementioned range, were omitted from Fig. 15 for the sake of visual clarity. The longer periods calculated herein in comparison with the estimation for Lisbon might be due to the non-consideration of the additional stiffness provided by structural elements such as stair cases, elevator shafts or eventual shear walls. Nonetheless, the periods of vibration estimated for Barcelona suggest a reasonable matching with the remaining pre-

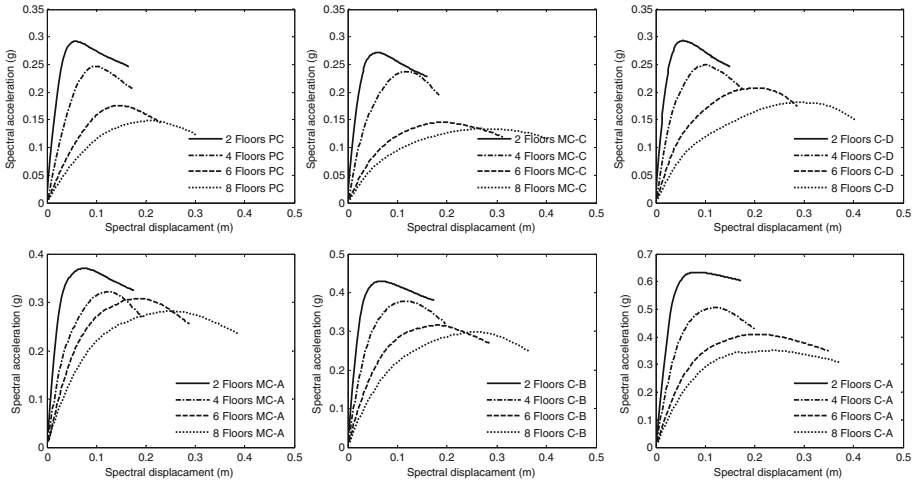

Fig. 16 Capacity curves for pre-code, mid-code (seismic zone C) and post-code (seismic zone D); and mid-code (seismic zone A), post-code (seismic zone B) and post-code (seismic zone A) building typologies; respectively upper (*left*, *middle* and *right*) and lower (*left*, *middle* and *right*) partial plots

dictions, given the observed relative differences with respect to the latter and the remaining cases.

3.1.2 Capacity curves

The global displacement and base shear capacities for each building typology were analysed. Thus, for each typology, a set of bare frames was randomly generated and used to derive several displacement-based adaptive pushover curves. Then, each pushover curve (top displacement vs. base shear for the multi degree-of-freedom system) was transformed into a capacity curve (spectral displacement vs. spectral acceleration for the equivalent single degree-of-freedom system), using the deformed shape of the frame at each step, as proposed by Casarotti and Pinho (2007). The mean capacity curves computed for pre-code (PC); mid-code, seismic zones C and A (MC-C and MC-A); and post-code, seismic zones D, B and A (C–D, C–B and C–A) typologies are depicted in Fig. 16. The latter refer to 2, 4, 6 and 8 floor building typologies, so as to provide a representative and visually clear illustration of the Portuguese building portfolio structural properties.

The results corresponding to pre-code, mid-code and post-code typologies are in agreement with the values of spectral acceleration estimated by Carvalho et al. (2002), in the cases for which direct comparison was possible, since the presently addressed seismic design zonation was not considered in the aforementioned study. However, capacity curves evaluated herein in accordance with provisions for zone A impart slightly higher lateral load resistance for both mid- and post-code typologies. This could be explained by the fundamentals of the mentioned benchmark study, which resorts to FEMA (1999) methodology and inherent seismic coefficient (seismic design resistance to building weight ratio) for the derivation of structural capacity expressed in the domain of spectral values of response. Despite the employment of engineering judgement to ensure the agreement of such parameters with the different construction epoch regulations, performed by Carvalho et al. (2002), the mentioned methodology embodies the shortcoming of being calibrated for buildings in the United States,

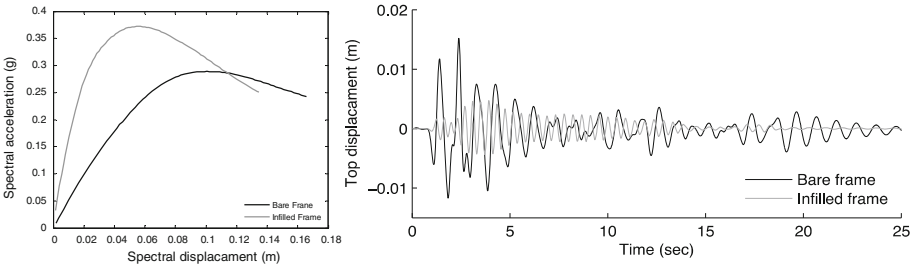

Fig. 17 Mean capacity curve for a sample of one hundred of pre-code frames with 4 storeys (*left*) and top displacement time-history of a single frame of the same building typology (*right*)

which differ from the Portuguese portfolio in terms of geometric, material and mechanical properties. In addition to the expected discrepancies related with the different methodologies employed in the development of the capacity curves, it is also worth mentioning that the lower displacement capacity estimated herein could also be due to the fact that a lower inter-story height was considered in this study, as well as P-delta effects, which tend to cause an earlier collapse in the frame.

The introduction of the infill panels induced an increase in the initial stiffness and overall strength, and consequently, a substantial decrease in the period of vibration by approximately 50 % (see Fig. 15). The influence of this feature in the structural capacity is demonstrated on Fig. 17, where the mean capacity curves for one hundred pre-code frames with four storeys (with and without the masonry infills) are depicted. For a randomly selected frame, a nonlinear dynamic analysis was also performed using the ground motion record from the 2007 Portuguese earthquake (magnitude of 5.8Mw and PGA of 0.04 g).

The variation between the structural and dynamic characteristics of the bare and infill frames seemed to be in agreement with recent studies (e.g. Dolšek and Fajfar 2008; Özcebe 2011; Uva et al. 2012).

3.2 Fragility functions

The selection of the ground motion parameter to represent each ground motion record is of fundamental importance, as each intensity measure type has a specific correlation with damage. Macroseismic intensities (e.g. MMI, EMS) could be a natural choice since there is a direct relationship between the intensity levels and the severity of damage in different building typologies. However, keeping track of the intensity at the location where the record was captured is not common and furthermore, macroseismic intensity does not take into account the influence of the frequency content on the structural response. Peak ground motion (e.g. PGA, PGV) also shares this latter shortcoming. The influence of the frequency content on the ground motion can be considered by choosing spectral acceleration or displacement to represent each record (e.g. Bommer et al. 2002). The period for which these spectral ordinates are computed also influences considerably the uncertainty in each limit state curve. In the European project Syner-G, more than four hundred fragility functions were collected (Crowley et al. 2014), and in those that adopted spectral ordinates, the elastic period (T_{el}) was the most common choice. In few cases, the employment of the yielding period (T_y) or the period at each limit state (T_{LSi}) was also observed. Using T_{el} might seem advantageous as it can be easily estimated (instrumentally or analytically), however the damage introduced in the structures even for weak motion (cracking of the concrete), causes an elongation of the

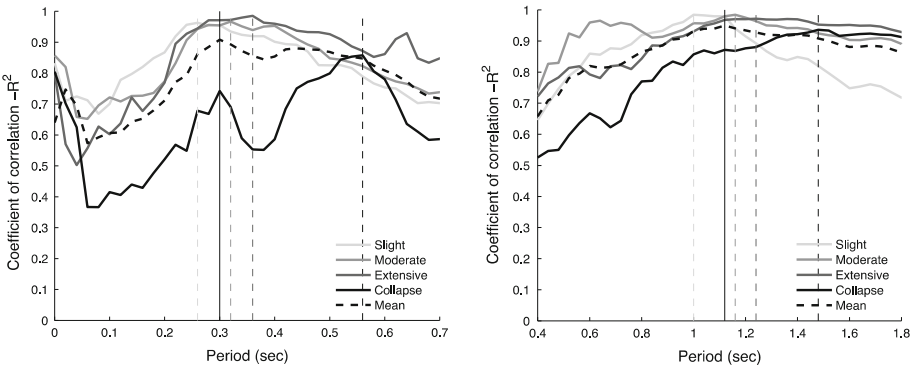

Fig. 18 Variation of the correlation between the intensity measure levels and the cumulative percentage of frames in each damage state for PC 2 storeys (*left*) and C >8 storeys (*right*) RC structures, as a function of the period

period of vibration, thus changing their dynamic properties. The coefficient of correlation (R^2) between the intensity measure levels and the cumulative percentage of frames for each limit state was estimated within a range of periods for each limit state for the 48 building typologies, and is illustrated in Fig. 18 for 2 storeys pre-code and 8-10 storeys post-code RC frames. The mean coefficient of correlation is also presented and the period for which the maximum correlation was observed for each limit state curve is marked with a vertical dashed line. The spectral acceleration for T_{el} seems to perform poorly, with a mean coefficient of correlation value of 0.60.

It is fair to state that the variation of the coefficient of correlation as a function of the period changes differently depending on the limit state. For slight or moderate damage, a smaller elongation of the period is observed due to a lower structural degradation of the frames and thus, a better correlation is observed for shorter periods. On the other hand, for extensive damage or collapse, a better performance is observed with longer periods, as frames sustaining such damage are likely to have their more variation in their dynamic properties. For the case of 2 storeys pre-code frames, the mean coefficient of correlation is considerably lower (0.66) for T_{el} (0.19 s) and reaches its maximum (0.92) for a value very close to the optimal period for the moderate damage limit state, which defines the threshold after which the frames begin to sustain plastic deformations (yielding point). This behaviour was also verified for the limit state curves of the remaining building typologies. For this reason, the authors decided to employ the spectral acceleration for the yielding period as the representative measure of each ground motion record. Moreover, (T_y) can be easily extracted from the capacity curves ($T_y = 2\pi\sqrt{Sd_y/Sa_y}$) or through the employment of simplified formulae (e.g. Crowley and Pinho 2004, 2006).

The cumulative percentage of frames exceeding each limit state at each ground motion record is presented in Fig. 19, along with the associated limit state curves derived from the scatter of points using the least squares method. As previously mentioned, a set of fragility curves has been developed according to each damage criterion: global drift or inter-story drift.

Each fragility function was assumed to follow a cumulative lognormal distribution, with logarithmic mean (λ) and logarithmic standard deviation (ζ). The results for all the building typologies according to the assumed damage criterion are described in Tables 6, 7 and 8.

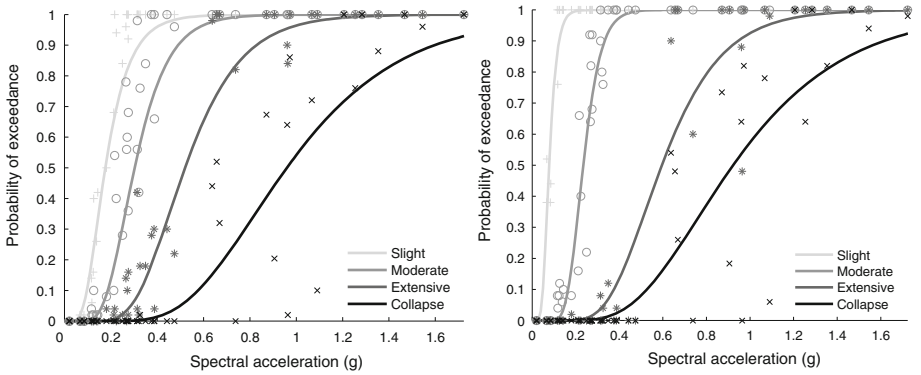

Fig. 19 Fragility model for pre-code low-rise RC buildings, considering the global drift (*left*) and inter-story drift (*right*) damage criteria

Table 6 Logarithmic mean (λ), logarithmic standard deviation (ζ) for the pre-code fragility functions

Damage criterion		Global drift				Inter-story drift			
Limit state		Slight	Moderate	Extensive	Collapse	Slight	Moderate	Extensive	Collapse
PC_1 $T_y = 0.23$ s	λ	−1.784	−1.331	−0.711	−0.284	−2.635	−1.440	−0.535	−0.130
	ζ	0.543	0.569	0.373	0.390	0.270	0.441	0.283	0.473
PC_2 $T_y = 0.30$ s	λ	−2.013	−1.522	−0.979	−0.284	−2.635	−1.440	−0.650	−0.130
	ζ	0.470	0.377	0.363	0.398	0.258	0.353	0.398	0.415
PC_3 $T_y = 0.45$ s	λ	−2.202	−1.584	−1.019	−0.378	−2.993	−1.740	−0.823	−0.299
	ζ	0.514	0.343	0.377	0.341	0.356	0.301	0.360	0.486
PC_4 $T_y = 0.60$ s	λ	−2.638	−2.145	−1.385	−0.926	−3.635	−2.377	−1.123	−0.253
	ζ	0.558	0.409	0.390	0.285	0.553	0.250	0.321	0.557
PC_5-7 $T_y = 0.80$ s	λ	−3.045	−2.237	−1.467	−1.088	−3.867	−2.152	−1.175	−0.737
	ζ	0.458	0.430	0.313	0.324	0.369	0.412	0.301	0.394
PC_ > 8 $T_y = 0110$ s	λ	−2.711	−2.144	−1.583	−1.180	−4.089	−2.512	−1.525	−0.712
	ζ	0.407	0.354	0.400	0.476	0.443	0.350	0.291	0.595

The appraisal of the coefficient of correlation throughout the various fragility functions indicates a lower dispersion of the data when adopting a global drift damage criterion, mainly for the first two limit state curves. This reduced scatter does not necessarily signify a lower variability in the vulnerability functions, as each limit state fragility function contributes differently to the resulting loss ratio. As demonstrated in Sect. 2.4, extensive damage and collapse limit state curves have a greater damage ratio, and will thus have a greater influence in the variability of the vulnerability curves.

3.3 Vulnerability functions

As mentioned in Sect. 2.2.3, after each nonlinear dynamic analysis, the residual inter-story drift was extracted and a statistical procedure employed to assess whether the frame should be demolished or repaired. This aspect is very important from a loss assessment point of view, as buildings with excessive residual drift are likely to be demolished, thus increasing the total loss. For this reason, another set of fragility functions was derived, considering

Table 7 Logarithmic mean (λ), logarithmic standard deviation (ζ) for the mid-code fragility functions

Zone	Limit state		Global drift				Inter-story drift			
			Slight	Moderate	Extensive	Collapse	Slight	Moderate	Extensive	Collapse
A	MC_A_1 $T_y = 0.24$ s	λ	−1.411	−0.901	−0.239	0.077	−2.031	−0.695	−0.028	0.610
		ζ	0.402	0.423	0.445	0.373	0.321	0.390	0.349	0.571
	MC_A_2 $T_y = 0.30$ s	λ	−1.739	−1.220	−0.718	0.080	−2.435	−1.194	−0.446	0.162
		ζ	0.378	0.337	0.365	0.346	0.318	0.365	0.295	0.369
	MC_A_3 $T_y = 0.45$ s	λ	−1.943	−1.311	−0.802	−0.098	−2.850	−1.525	−0.633	0.012
		ζ	0.367	0.293	0.333	0.465	0.338	0.303	0.300	0.459
	MC_A_4 $T_y = 0.60$ s	λ	−2.122	−1.365	−0.885	−0.261	−3.237	−1.729	−0.765	−0.070
		ζ	0.456	0.348	0.341	0.383	0.358	0.341	0.304	0.450
	MC_A_5-7 $T_y = 0.80$ s	λ	−2.326	−1.645	−1.086	−0.582	−3.328	−1.887	−0.857	−0.222
		ζ	0.462	0.523	0.275	0.228	0.378	0.283	0.347	0.425
	MC_A_>8 $T_y = 1.10$ s	λ	−2.136	−1.623	−0.988	−0.404	−3.613	−2.110	−1.167	−0.169
		ζ	0.290	0.446	0.421	0.375	0.314	0.350	0.294	0.387
B	MC_B_1 $T_y = 0.23$ s	λ	−1.620	−1.065	−0.338	0.036	−2.054	−0.718	−0.190	0.341
		ζ	0.356	0.369	0.369	0.388	0.380	0.365	0.392	0.478
	MC_B_2 $T_y = 0.30$ s	λ	−1.865	−1.374	−0.785	−0.080	−2.485	−1.242	−0.502	0.011
		ζ	0.373	0.420	0.335	0.432	0.250	0.353	0.351	0.397
	MC_B_3 $T_y = 0.45$ s	λ	−2.054	−1.415	−0.894	−0.215	−2.868	−1.528	−0.665	−0.049
		ζ	0.345	0.335	0.290	0.484	0.335	0.304	0.392	0.383
	MC_B_4 $T_y = 0.60$ s	λ	−2.211	−1.533	−0.945	−0.282	−3.340	−1.814	−0.833	−0.090
		ζ	0.316	0.296	0.345	0.451	0.521	0.354	0.372	0.366
	MC_B_5-7 $T_y = 0.80$ s	λ	−2.414	−1.794	−1.140	−0.747	−3.438	−1.992	−1.005	−0.459
		ζ	0.280	0.446	0.421	0.375	0.214	0.350	0.294	0.287
	MC_B_>8 $T_y = 1.10$ s	λ	−2.459	−1.769	−1.147	−0.751	−3.650	−2.283	−1.244	−0.412
		ζ	0.384	0.416	0.462	0.492	0.222	0.325	0.307	0.441

Table 7 continued

Zone	Limit state		Global drift				Inter-story drift			
			Slight	Moderate	Extensive	Collapse	Slight	Moderate	Extensive	Collapse
C	MC_C_1 $T_y = 0.23$ s	λ	−1.898	−1.465	−0.865	−0.308	−2.760	−1.389	−0.536	−0.225
		ζ	0.449	0.453	0.268	0.266	0.366	0.390	0.300	0.426
	MC_C_2 $T_y = 0.30$ s	λ	−2.087	−1.624	−1.034	−0.312	−2.828	−1.737	−0.799	−0.300
		ζ	0.337	0.405	0.347	0.388	0.299	0.383	0.416	0.366
	MC_C_3 $T_y = 0.45$ s	λ	−2.295	−1.771	−1.227	−0.568	−3.172	−1.820	−0.915	−0.302
		ζ	0.301	0.327	0.316	0.428	0.348	0.308	0.304	0.418
	MC_C_4 $T_y = 0.60$ s	λ	−2.939	−2.358	−1.735	−1.237	−3.915	−2.446	−1.384	−0.796
		ζ	0.265	0.248	0.284	0.468	0.497	0.292	0.292	0.370
	MC_C_5-7 $T_y = 0.80$ s	λ	−2.950	−2.271	−1.463	−1.139	−3.883	−2.548	−1.288	−0.851
		ζ	0.345	0.338	0.335	0.379	0.369	0.401	0.391	0.447
	MC_C_>8 $T_y = 1.1$ s	λ	−2.782	−2.159	−1.583	−1.255	−4.165	−2.475	−1.557	−1.071
		ζ	0.488	0.386	0.502	0.609	0.231	0.300	0.321	0.594

Table 8 Logarithmic mean (λ), logarithmic standard deviation (ζ) for the post-code fragility functions

Zone	Limit state		Global drift				Inter-story drift			
			Slight	Moderate	Extensive	Collapse	Slight	Moderate	Extensive	Collapse
A	C_A_1 $T_y = 0.23$ s	λ	−1.105	−0.618	−0.004	0.454	−1.870	−0.458	0.157	0.919
		ζ	0.411	0.364	0.292	0.401	0.454	0.354	0.391	0.512
	C_A_2 $T_y = 0.30$ s	λ	−1.075	−0.669	−0.125	0.680	−2.125	−0.790	0.135	0.946
		ζ	0.275	0.396	0.296	0.416	0.373	0.206	0.419	0.624
	C_A_3 $T_y = 0.45$ s	λ	−1.752	−1.222	−0.591	0.326	−2.765	−1.367	−0.335	0.654
		ζ	0.284	0.340	0.320	0.628	0.288	0.359	0.376	0.643
	C_A_4 $T_y = 0.60$ s	λ	−2.060	−1.152	−0.764	−0.112	−3.148	−1.485	−0.564	0.022
		ζ	0.293	0.484	0.344	0.450	0.253	0.313	0.333	0.462
	C_A_5-7 $T_y = 0.80$ s	λ	−2.153	−1.475	−0.787	−0.399	−3.117	−1.755	−0.655	0.030
		ζ	0.375	0.375	0.367	0.458	0.493	0.425	0.448	0.356
	C_A_>8 $T_y = 1.10$ s	λ	−1.967	−1.301	−0.714	−0.250	−3.496	−1.956	−0.746	0.337
		ζ	0.314	0.312	0.370	0.355	0.253	0.326	0.284	0.672
B	C_B_1 $T_y = 0.23$ s	λ	−1.171	−0.637	−0.085	0.199	−1.933	−0.466	0.121	0.865
		ζ	0.334	0.330	0.298	0.335	0.372	0.369	0.345	0.350
	C_B_2 $T_y = 0.30$ s	λ	−1.597	−1.130	−0.649	0.155	−2.374	−1.118	−0.321	0.245
		ζ	0.325	0.362	0.342	0.421	0.414	0.298	0.350	0.405
	C_B_3 $T_y = 0.45$ s	λ	−1.873	−1.246	−0.706	0.011	−2.773	−1.420	−0.476	0.071
		ζ	0.325	0.362	0.342	0.421	0.414	0.298	0.350	0.405
	C_B_4 $T_y = 0.60$ s	λ	−2.066	−1.278	−0.792	−0.167	−3.178	−1.616	−0.630	0.009
		ζ	0.250	0.378	0.364	0.370	0.283	0.320	0.290	0.443
	C_B_5-7 $T_y = 0.80$ s	λ	−2.259	−1.567	−0.858	−0.490	−3.142	−1.824	−0.655	0.020
		ζ	0.412	0.402	0.529	0.593	0.451	0.364	0.616	0.691
	C_B_>8 $T_y = 1.10$ s	λ	−2.067	−1.469	−0.834	−0.325	−3.532	−2.027	−0.846	0.237
		ζ	0.283	0.282	0.407	0.457	0.286	0.255	0.345	0.611

Table 8 continued

Zone	Limit state		Global drift				Inter-story drift			
			Slight	Moderate	Extensive	Collapse	Slight	Moderate	Extensive	Collapse
C	C_C_1 $T_y = 0.23$ s	λ	−1.426	−0.869	−0.263	0.104	−1.981	−0.645	−0.005	0.406
		ζ	0.406	0.427	0.362	0.450	0.238	0.364	0.254	0.605
	C_C_2 $T_y = 0.30$ s	λ	−1.712	−1.202	−0.665	0.122	−2.429	−1.147	−0.398	0.120
		ζ	0.386	0.398	0.277	0.449	0.093	0.359	0.307	0.449
	C_C_3 $T_y = 0.45$ s	λ	−1.939	−1.334	−0.790	−0.097	−2.804	−1.473	−0.589	0.037
		ζ	0.361	0.359	0.306	0.436	0.305	0.331	0.341	0.456
	C_C_4 $T_y = 0.60$ s	λ	−2.100	−1.348	−0.850	−0.210	−3.199	−1.692	−0.740	−0.028
		ζ	0.337	0.321	0.336	0.424	0.517	0.302	0.376	0.463
	C_C_5-7 $T_y = 0.80$ s	λ	−2.329	−1.678	−1.043	−0.552	−3.383	−1.923	−0.830	−0.271
		ζ	0.508	0.353	0.360	0.361	0.292	0.250	0.306	0.463
	C_C_>8 $T_y = 1.10$ s	λ	−2.312	−1.703	−1.050	−0.531	−3.585	−2.201	−1.130	−0.135
		ζ	0.385	0.299	0.458	0.491	0.298	0.269	0.394	0.486
D	C_D_1 $T_y = 0.23$ s	λ	−1.776	−1.353	−0.663	−0.155	−2.654	−1.317	−0.428	−0.044
		ζ	0.345	0.360	0.377	0.425	0.280	0.318	0.297	0.353
	C_D_2 $T_y = 0.30$ s	λ	−1.985	−1.570	−0.888	−0.210	−2.692	−1.571	−0.673	−0.209
		ζ	0.345	0.360	0.377	0.425	0.280	0.318	0.297	0.353
	C_D_3 $T_y = 0.45$ s	λ	−2.043	−1.570	−0.980	−0.243	−2.989	−1.584	−0.673	−0.209
		ζ	0.308	0.304	0.323	0.421	0.291	0.306	0.358	0.311
	C_D_4 $T_y = 0.60$ s	λ	−2.429	−1.823	−1.057	−0.692	−3.453	−2.153	−0.806	−0.068
		ζ	0.271	0.282	0.369	0.417	0.402	0.295	0.320	0.369
	C_D_5-7 $T_y = 0.80$ s	λ	−2.452	−1.756	−1.262	−0.836	−3.401	−1.971	−0.977	−0.438
		ζ	0.418	0.288	0.340	0.319	0.271	0.419	0.387	0.426
	C_D_>8 $T_y = 1.10$ s	λ	−2.556	−1.861	−1.165	−0.713	−3.787	−2.376	−1.268	−0.507
		ζ	0.486	0.315	0.509	0.524	0.209	0.284	0.344	0.361

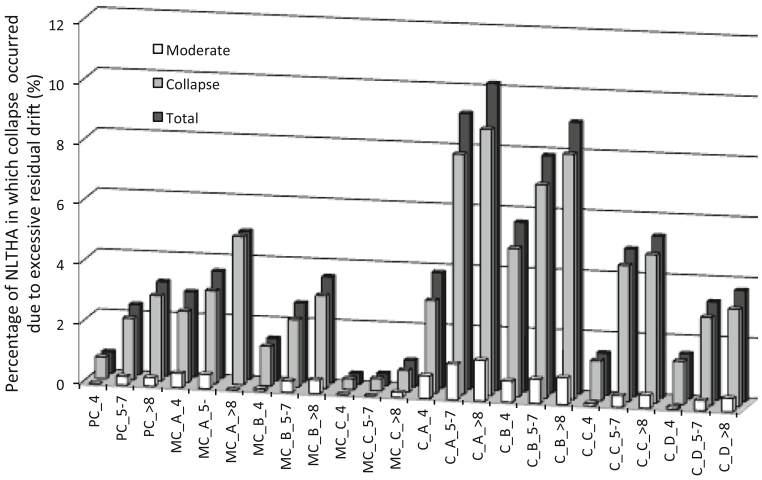

Fig. 20 Percentage of nonlinear dynamic analysis (per damage state and in total), in which collapse occurred due to excessive residual inter-story drift

this additional amount of frames that should be defined as collapsed, rather than sustaining moderate or extensive damage. In Fig. 20, the percentage of nonlinear dynamic analysis in which a frame was classified as collapsed due to excessive residual inter-story drift is presented for each building typology.

The cases of collapse due to residual drift were observed more often in frames with a higher number of storeys, and only when moderate or extensive damage was attained. This aspect does not influence the slight or moderate limit state curves, as the cumulative number of frames under each limit state remains the same. It does, however, have a direct impact on the extensive damage or collapse curves, as the number of frames with at least such a level of damage will increase. Higher levels of residual deformations in post-code frames, rather than in pre-code ones, were also observed. This greater likelihood of occurrence of permanent drifts in systems capable of withstanding large displacements is also indicated Ramirez and Miranda (2012).

In Fig. 21, a set of fragility functions for pre-code high-rise RC frames is presented with and without the consideration of the impact of excessive residual inter-story drift.

After the computation of the fragility model considering this feature, the consequence model described in Sect. 2.4 was used to derive vulnerability functions. In this process, for a set of intensity measure levels, the percentage of buildings in each damage state are computed and multiplied by the respective damage ratio, thus obtaining a loss ratio for each intensity measure level. The consideration of the large spectrum of uncertainties considered in this study, impose a significant variability of loss ratio at each intensity measure level. In order to evaluate this uncertainty, a statistical method was implemented that allowed the estimation of the 10 and 90 % percentiles. This method consists of a continuous bootstrap sampling with replacement from the original dataset (e.g. Wasserman 2004). The resulting mean vulnerability functions and associated percentiles are depicted in Fig. 22, for the global drift (black) and inter-story drift (grey) damage criteria.

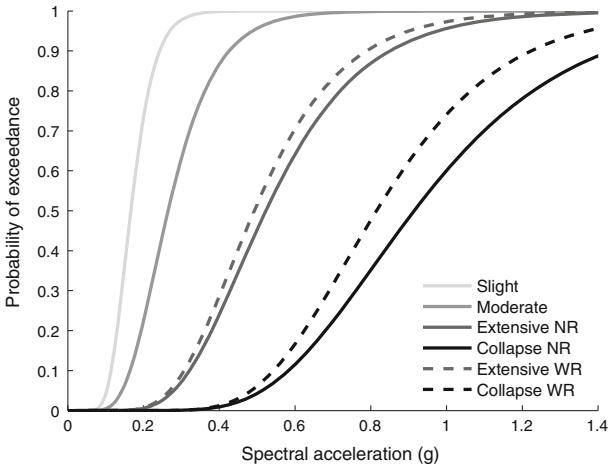

Fig. 21 Fragility model for pre-code high-rise RC frames with (WR) and without (NR) considering collapse due to excessive residual inter-story drift

4 Conclusions

The structural characteristics of typical Portuguese reinforced concrete buildings were thoroughly examined in this study. Hundreds of building drawings from different regions in Portugal were collected and analysed with the purpose of deriving the statistical distribution of a set of geometrical properties. These results can be used to carry out investigations regarding the seismic vulnerability of the RC building stock in Portugal, or employed directly in seismic risk methodologies such as the Displacement-Based Earthquake Loss Assessment (DBELA) (Crowley et al. 2004; Bal et al. 2010). Despite the useful contribution that this statistical study might provide to future endeavours in the area of the vulnerability assessment of the Portuguese building stock, it is clear by the number of failed Chi-square tests, that the size of the analysed sample of RC buildings needs to be further increased. Furthermore, it is also important to recognize that the results presented herein are based on the observations of the drawings and technical specifications, which might vary from what has been built in reality. Finally, the Authors would like to emphasise that the RC population investigated in this study was composed uniquely by regular moment frame structures, and therefore, the influence of stiff elements like elevator shafts or shear walls was neglected.

The geometric and material probabilistic distributions were employed to generate hundreds of RC frames through Monte Carlo simulation, representative of 48 building typologies, organized according to their number of storeys, design code level and seismic zonation. The dynamic and structural characteristics of these frames were compared, and it was concluded that a fair agreement existed between previous analytical and empirical studies. A sample of one hundred frames was tested against one hundred ground motion records, leading to ten thousand nonlinear dynamic analyses for each building typology. For each analysis, the global drift and the inter-story drift were employed to allocate each frame in a damage state, according to a five level damage scale (none, slight, moderate, extensive and collapse). For each damage criterion, a fragility model was derived for the 48 building typologies, using spectral acceleration for the yield period as the representative measurement of the ground motion. Taking into consideration the eventual demolition due to excessive residual inter-

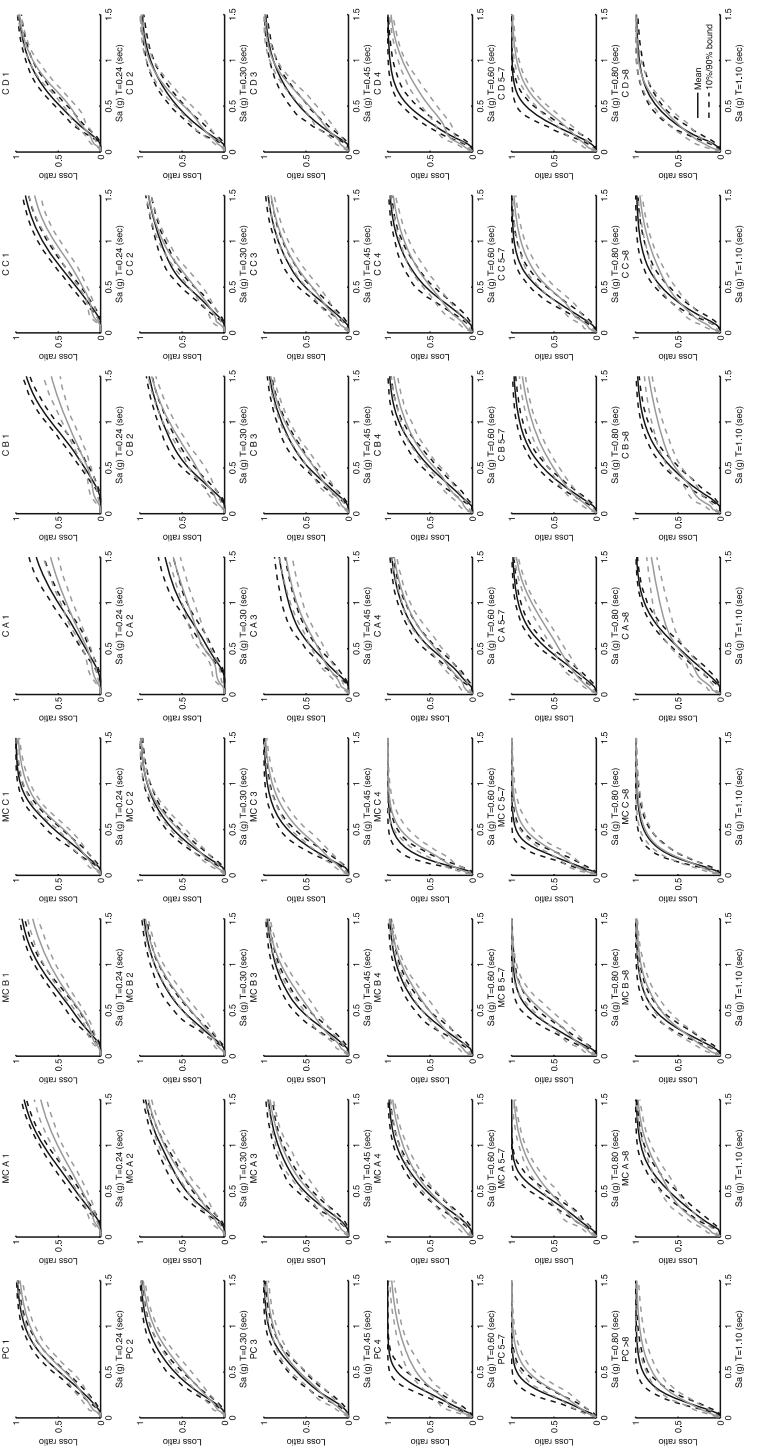

Fig. 22 Vulnerability model for RC building in Portugal assuming a global drift (*black*) and an inter-story drift (*grey*) damage criteria

story drift, a second set of fragility functions were also created. The consideration of the residual inter-story drifts caused a considerable increase in the extensive and collapse limit state curves for mid-rise and high-rise building typologies, but no significant changes in the low-rise fragility functions. This second set of fragility functions was combined with a consequence model to derive a vulnerability model.

The distribution of the loss ratios at each intensity measure level was evaluated through the employment of a bootstrap method, allowing the estimating of 10 and 90 % percentile curves. An increase was observed in the probability of loss for the building classes designed before the implementation of the first seismic code (pre-code), or designed according to a seismic zone characterized by low seismicity. Furthermore, the vulnerability functions produced using the maximum inter-story drift seemed to lead to higher loss ratios at low intensity measure levels. This aspect could be due to the fact that in the adaptation of the original scale proposed by Rossetto and Elnashai (2003) to the one considered herein, "slight" and "light" damage states were merged into one, and combined with a damage ratio of 10 %. Such ratio might be excessively high for the first damage state of this scale. Nevertheless, a fair agreement is observed between the vulnerability functions from each damage criterion for low- and mid-rise building typologies. With regards to the uncertainty in the loss ratio, a similar variability was obtained regardless of the chosen damage criterion.

The results obtained herein were employed in a probabilistic seismic risk assessment for mainland Portugal, as described in Silva et al. (2014a). The two sets of vulnerability functions were included within a logic tree framework, thus allowing a better characterization of the epistemic uncertainty in the vulnerability. The seismic hazard and risk calculations were carried using the OpenQuake engine (Silva et al. 2013), the open-source code for seismic hazard and risk assessment currently being developed by the Global Earthquake Model [GEM (http://www.globalquakemodel.org/)] initiative.

Acknowledgments The authors are grateful to the various representatives of the public and private institutions that facilitated the access to the drawings and technical specifications of RC buildings. The authors would also like to express their gratitude to Dr. Manuel Pipa, Dr. Hugo Rodrigues, Dr. Catarina Fernandes and José Melo for their valuable contribution in the investigation of the material characteristics and Romain Sousa for the important suggestions in the structural modelling process. Part of this work has been performed within the framework of the research project PTDC/ECM-EST/3062/2012 'Earthquake loss of the Portuguese building stock' funded by the Foundation of Science and Technology (FCT) of Portugal.

References

Akkar S, Sucuoglu H, Yakut A (2005) Displacement-based fragility functions for low- and mid-rise ordinary concrete buildings. Earthq Spectra 21(4):901–927

Almunia JAS (1993) Evaluación del comportamiento funcional y de la seguridad estructural de puentes existentes de hormigón armado y pretensado. Tesis Doctoral. Escola Técnica Superior D'Enginyers de Camins, Canals I Ponts, Universitat Politècnica de Catalunya, Barcelona, Spain (in Spanish)

Antoniou S, Pinho R (2004b) Development and verification of a displacement-based adaptive pushover procedure. J Earthq Eng 8(5):643–661

Bal IE, Crowley H, Pinho R, Gulay F (2008) Detailed assessment of structural characteristics of Turkish RC building stock for loss assessment models. Soil Dyn Earthq Eng 28:914–932

Bal IE, Crowley H, Pinho R (2010) "Displacement-based earthquake loss assessment: Method development and application to Turkish building stock", ROSE Research Report 2010/02. IUSS Press, Pavia

Bommer JJ, Spence R, Erdik M, Tabuchi S, Aydinoglu N, Booth E, Re DD, Pterken D (2002) Development of an earthquake loss model for Turkish catastrophe insurance. J Seismol 6:431–446

Borzi B, Pinho R, Crowley H (2008) Simplified pushover-based vulnerability analysis for large-scale assessment of RC buildings. Eng Struct 30:804–820

Calvi GM, Pinho R (2004) LESSLOSS—a European integrated project on risk mitigation for earthquakes and landslides. IUSS Press, Pavia

Campos Costa A, Sousa ML, Carvalho A, Coelho E (2009) Evaluation of seismic risk and mitigation strategies for the existing building stock: application of LNECloss to the metropolitan area of Lisbon. Bull Earthq Eng 8:119–134

Carvalho EC, Coelho E (2001) Seismic assessment, strengthening and repair of structures, ECOEST2-ICONS report no. 2, European Commission—Training and Mobility of Researchers Programme

Carvalho EC, Coelho E, Campos Costa A, Sousa ML, Candeias P (2002) Vulnerability evaluation of residential buildings in Portugal. In: Proceedings of the 12th European conference on earthquake engineering, London, UK

Casarotti C, Pinho R (2007) An adaptive capacity spectrum method for assessment of bridges subjected to earthquake action. Bull Earthq Eng 5(3):377–390

CEN (2004) Eurocode 2: design of concrete structures. European Committee for Standardization, Brussels, Belgium

CEN (2005) Eurocode 8: design of structures for earthquake resistance. European Committee for Standardization, Brussels, Belgium

Coburn A, Spence R (2002) Earthquake protection, 2nd edn. Wiley andSons.

Crowley H, Pinho R (2004) Period-height relationship for existing European reinforced concrete buildings. J Earthq Eng 8:893–119

Crowley H, Pinho R (2006) Simplified equations for estimating the period of vibration of existing buildings. In: Proceedings of the 1st European conference on earthquake engineering and seismology, Geneva, Switzerland, Paper No. 1122

Crowley H, Pinho R, Bommer J (2004) A probabilistic displacement-based vulnerability assessment procedure for earthquake loss estimation. Bull Earthq Eng 2:173–219

Crowley H, Colombi M, Silva V (2014) Chapter 4: epistemic uncertainty in fragility functions for European RC buildings. In: SYNER-G: typology definition and fragility functions for physical elements at seismic risk: buildings, lifelines, transportation networks and critical facilities. Ed: Pitilakis, Crowley, Kaynia (in press)

Dawe JL, Seah CK (1988) Lateral load resistance of masonry panels in flexible steel frames. In: Proceedings of the 8th international brick and block masonry conference, Dublin, Ireland

Di Pasquale G, Goretti A (2001) Vulnerabilità funzionale ed economica degli edifici residenziali colpiti dai recenti eventi sismici italiani. Proceedings of the 10^{th} national conference "L'ingegneria Sismica in Italia", Potenza-Matera, Italy

Dolšek M, Fajfar P (2008) The effect of masonry infills on the seismic response of a four story reinforced concrete frame—a deterministic assessment. Eng Struct 30(7):1991–2001

Enomoto T, Schmitz M, Abeki N, Masaki K, Navarro M, Rocavado V, Sanchez A (2000) Seismic risk assessment using soil dynamics in Caracas, Venezuela. In: Proceedings of the 12th World conference in earthquake engineering, Auckland, New Zealand

Erberik MA (2007) Fragility-based assessment of typical mid-rise and low-rise RC buildings in Turkey. Eng Struct 30(5):1360–1374

Erberik MA (2008) Fragility-based assessment of typical mid-rise and low-rise RC buildings in Turkey. Eng Struct 30(5): 1360–1374

Espinoza F (1999) Determinación de las características dinámicas de estructuras. Ph.D. Thesis, Universidad Politécnica de Catalunya, Barcelona, Spain

Fajfar P (1999) Capacity spectrum method based on inelastic demand spectra. Earthq Eng Struct Dyn 28(9):979–993

FEMA and NIBS (1999) Earthquake loss estimation methodology—HAZUS 99. Federal Emergency Management Agency and National Institute of Buildings Sciences, Washington, DC, USA

FEMA-273 (1997) NEHRP guidelines for the seismic rehabilitation of buildings. Report No. FEMA 273. Federal Emergency Management Agency, Washington, DC, USA

FEMA-443 (2003) HAZUS-MH technical manual. Federal Emergency Management Agency, Washington DC, USA

Fernandes C, Melo J, Varum H, Costa A (2011) Comparative analysis of the cyclic behavior of beam-column joints with plain and deformed reinforcing bars. IBRACON Struct Mater J 4(1):147–172

Freeman S (2004) Review of the development of the capacity spectrum method. ISET J Earthq Technol 41:1–13

Giuffrè A, Pinto PE (1970) Il comportamento del cemento armato per sollecitazioni cicliché di forte intensità, Giornale del Génio Civile (in Italian)

Hancilar U, Durukal E, Franco G, Deodatis G, Erdik M, Smyth A (2006) Probabilistic vulnerability analysis: an application to a typical school building in Istanbul. In: Proceedings of the 1st European conference on earthquake engineering and seismology, Geneva, Switzerland, Paper No. 889

Hashemi A, Mosalam K (2007) Seismic evaluation of reinforced concrete buildings including effects of masonry infill walls. PEER Report 2007/100, Pacific Earthquake Engineering Research Center,University of California, Berkeley, USA
Kappos A, Panagopoulos G, Panagiotopoulos C, Penelis G (2006) A hybrid method for the vulnerability assessment of R/C and URM buildings. Bull Earthq Eng 4(4):391–413
Kirçil M, Polat Z (2006) Fragility analysis of mid-rise R/C frame buildings. Eng Struct 28(9):1335–1345
Kobayashi H, Vidal F, Feriche D, Samano T, Alguacil G (1996) Evaluation of dynamic behaviour of building structures with microtremors for seismic microzonation mapping. In: Proceedings of the 11th world conference in earthquake engineering, Acapulco, México
Lagomarsino S, Giovinazzi S (2006) Macroseismic and mechanical models for the vulnerability assessment of current buildings. Bull Earthquake Eng, 4:415–443
Lopes L (2012) Dificuldades práticas na avaliação da segurança sísmica de estruturas existentes, MSc Thesis, University of Aveiro, Aveiro, Portugal (in Portuguese)
Melo J, Varum H, Rossetto T, Costa A (2012) Experimental response of RC columns built with plain bars under unidirectional cyclic loading. In: Proceedings of the 15th world conference on earthquake engineering, Lisbon, Portugal
Mouroux P, Le Brun BT (2006) Presentation of RISK-UE project. Bull Earthq Eng 4:323–339
Navarro M, Oliveira CS (2004) Evaluation of dynamic characteristics of reinforced concrete buildings in the City of Lisbon. In: Proceedings of the 4th assembly of the Portuguese–Spanish of geodesy and geophysics, Figueira da Foz, Portugal
NZSEE (2006) Assessment and improvement of the structural performance of buildings in earthquakes. New Zealand Society for Earthquake Engineering, Study Group Draft
Oliveira CS, Navarro M (2010) Fundamental periods of vibration of RC buildings in Portugal from in-situ experimental and numerical techniques. Bull Earthq Eng 8:609–642
Özcebe S (2011) Identification of initial damage states in displacement-based assessment of existing RC buildings. MSc Thesis, ROSE School, Pavia, Italy
Papaila A (2011) Seismic fragility curves for reinforced concrete buildings, MSc Thesis, University of Patras, Patras, Greece
Peláez Montilla JA, López Casado C (2002) Deaggregation in magnitude, distance, and azimuth in the south and west of the Iberian Peninsula. Bull Seismol Soc Am 92:2177–2185
Pipa M (1993) Ductilidade de Elementos de Betão Armado Sujeitos a Acções Cíclicas—Influência das Características Mecânicas das Armaduras. IST/LNEC, Lisbon, Portugal (in Portuguese)
Ramirez CM, Miranda E (2012) Significance of residual drifts in building earthquake loss estimation. Earthq Eng Struct Dyn 41:1477–1493
RBA (1935) Regulamento para o Emprego de Betão Armado, Decreto-Lei n° 4036, Lisbon, Portugal
REBA (1967) Regulamento de Estruturas de Betão Armado, Decreto-Lei n° 47723, Lisbon, Portugal
RGEU (2007) Regulamento Geral das Edificações Urbanas, Decreto-Lei n° 38382, Lisbon, Portugal
Rodrigues H, Varum H, Costa A (2010) Simplified macro-model for infill masonry panels. J Earthq Eng 14:390–416
Rodrigues H, Arêde A, Varum H, Costa AG (2012) Experimental evaluation of rectangular reinforced concrete column behaviour under biaxial cyclic loading. Earthq Eng Struct Dyn. doi:10.1002/eqe.2205
Rossetto T, Elnashai A (2003) Derivation of vulnerability functions for European-type RC structures based on observational data. Eng Struct 25(10):1241–1263
Rossetto T, Elnashai A (2005) A new analytical procedure for the derivation of displacement-based vulnerability curves for populations of RC structures. Eng Struct 27(3):397–409
RSA (1983) Regulamento de Segurança e Acções para Estruturas de Edifícios e Pontes, Decreto-Lei n.°235/83, Lisbon, Portugal
RSCCS (1958) Regulamento de Segurança das Construções Contra os Sismos, Decreto-Lei n°41658, Lisbon, Portugal
RSEP (1961) Regulamento de Solicitações em Edifício e Pontes, Decreto-Lei n.°44041, Lisbon, Portugal
Sattar S, Liel A (2010) Seismic Performance of the Reinforced Concrete Frame Structures with and without Masonry Infill Walls. In: Proceedings of the 9th US national and 10th Canadian conference on earthquake engineering, Toronto, Canada
Scott BD, Park R, Priestley MJN (1982) Stress–strain behavior of concrete confined by overlapping hoops at low and high strain rates. ACI J Proc 79(1):13–27
Silva V, Crowley H, Pagani M, Modelli D, Pinho R (2013) Development of the OpenQuake engine, the Global Earthquake Model's open-source software for seismic risk assessment. Nat Hazards. doi:10.1007/s11069-013-0618-x
Silva V, Crowley H, Varum H, Pinho R (2014a) Seismic hazard and risk assessment for mainland Portugal. Bull Earthq Eng. doi:10.1007/s10518-014-9630-0

Silva V, Crowley H, Pinho R, Varum H, Sousa R (2014b) Evaluation of analytical methodologies to derive vulnerability functions. Earthq Eng Struct Dyn. doi:10.1002/eqe.2337
Smyrou E, Blandon-Uribe C, Antoniou S, Pinho R, Crowley H (2006) Implementation and verification of a masonry panel model for nonlinear dynamic analysis of infilled frames. In: Proceedings of the first European conference on earthquake engineering and seismology, Geneva, Switzerland
Soares F (2012) Comportamento mecânico de alvenaria. A influência de abertura de roços (in portuguese). MSc Thesis of the University of Aveiro, Aveiro, Portugal
Sousa ML, Costa AC (2009) Ground motion scenarios consistent with probabilistic seismic hazard disaggregation analysis. Application to Mainland Portugal. Bull Earthq Eng 7:127–147
Spence R (2007) Earthquake disaster scenario prediction and loss modeling for urban areas. LESSLOSS Report—2007/07, IUSS Press, Pavia, Italy
Stafford-Smith B, Carter C (1969) A method for the analysis of infilled frames. Proc ICE 44:31–48
Uva G, Porco F, Fiore A (2012) Appraisal of masonry infill walls effect in the seismic response of RC framed buildings: a case study. Eng Struct 34:514–526
Vamvatsikos D, Cornell AC (2002) Incremental dynamic analysis. Earthq Eng Struct Dyn 31(3):491–514

Web References

Vargas YF, Pujades LB, Barbat AH (2010) Probabilistic assessment of the global damage in reinforced concrete structures. In: Proceedings of the 14th European conference on earthquake engineering, Ohrid, Macedonia
Vicente R (2004) Patologia das paredes de fachada. Estudo do comportamento mecânico das paredes de fachada com correcção exterior das pontes térmicas (in portuguese). MSc Thesis of the University of Coimbra, Coimbra, Portugal
Vilanova S, Fonseca J (2007) Probabilistic seismic-hazard assessment for Portugal. Bull Seismol Soc Am 97:1702–1717
Wasserman L (2004) All of statistics: a concise course on statistical inference. Springer, New York
Portuguese Census Survey 2011: http://censos.ine.pt/
PEER strong motion database: http://peer.berkeley.edu/smcat/
European strong motion database: http://www.isesd.hi.is/
French Accelerometric Network: http://www-rap.obs.ujf-grenoble.fr/
Swiss Earthquake Database: http://seispc2.ethz.ch/strong_motion/home.jsp
Matlab:http://www.mathworks.com/
OpenSEES: http://opensees.berkeley.edu/
Global Earthquake Model: http://www.globalquakemodel.org/